Econometrics and Statistics xxx (xxxx) xxx

Contents lists available at ScienceDirect

Econometrics and Statistics

journal homepage: www.elsevier.com/locate/ecosta

Risk Assessment and Spurious Seasonality

Malte S. Kurz[a,*], Stefan Mittnik[b,c]

[a] TUM School of Management, Technical University of Munich, Arcisstr. 21, 80333 Munich, Germany
[b] Department of Statistics, Ludwig-Maximilians-Universität München, Akademiestr. 1, 80799 Munich, Germany
[c] Scalable Capital, Seitzstr. 8e, 80538 Munich, Germany

ARTICLE INFO

Article history:
Received 1 December 2021
Revised 17 May 2022
Accepted 3 July 2022
Available online 8 July 2022

Keywords:
Autocorrelation function
Basel III
GARCH
Overlapping data
Temporal aggregation

ABSTRACT

To determine the appropriate level of risk capital, financial institutions are required to empirically estimate and predict specific risk measures. Although regulation commonly prescribes the forecasting horizon and the frequency with which risk assessments have to be reported, the scheme with which the underlying data are sampled typically remains unspecified. It is shown that, given assessment frequency and forecasting horizon, the choice of the sampling scheme can greatly affect the outcome of risk assessment procedures. Specifically, sequences of variance estimates are prone to exhibit spurious seasonality when the assessment frequency is higher than the sampling frequency of non-overlapping asset return data. The autocorrelation function of such sequences is derived for a general class of weak white noise processes and for a general class of variance estimators. The problem of spurious seasonality can be overcome by using overlapping return data for estimation of risk measures.

1. Introduction

Reliable estimation and prediction of the risk of financial instruments is key to sound financial risk management. In this paper, we address consequences of assessing risk for horizons that exceed the assessment frequency. This is commonly the case when asset managers rebalance weekly or monthly but assess and report risk at a daily frequency, situations that arise in banking (Basel III) and insurance (Solvency II) regulation. According to the Basel Committee on Banking Supervision (BCBS, 2016; 2019), for example, in Basel III, banks have to estimate the ten-day-ahead expected shortfall, i.e., the conditional loss expectation given that a predefined value-at-risk level is exceeded, on a daily basis.

In practice, the time interval over which returns are measured, the forecasting horizon and the frequency with which assessments take place are all specified by regulation or management policies. Typically, however, the sampling frequency of the data underlying the empirical analysis remains unspecified. For example BCBS (2016, §181 c) and BCBS (2019, MAR 33.4) state that the required ten-day expected shortfall estimates need to be derived without scaling from shorter horizons and allow using overlapping return data. Various studies have investigated possible consequences of using overlapping returns for risk estimation or, more general, for statistical inference (see, for example, Bod et al. (2002), Britten-Jones et al. (2011),

* Corresponding author.
E-mail addresses: malte.kurz@tum.de (M.S. Kurz), finmetrics@stat.uni-muenchen.de (S. Mittnik).

https://doi.org/10.1016/j.ecosta.2022.07.003

Fig. 1. Illustration of different combinations of return intervals and sampling schemes for deriving h-day-ahead risk measures. Each panel consists of two rows: The first row sketches the data used for estimation of h-day-ahead risk measure $RM_{t+h|t}$ at time t and the second row those at $t+1$ for risk measure $RM_{t+h+1|t+1}$. Panel (a) shows a scheme with daily sampling of daily returns. Here, risk estimates need to be scaled up to derive h-day-ahead risk estimates. Panel (b) illustrates the sampling scheme when using overlapping h-day returns. Panel (c) indicates the scheme when using non-overlapping h-day returns.

Daníelsson et al. (2016), Hansen and Hodrick (1980), Hedegaard and Hodrick (2016), Kluitman and Franses (2002), Mittnik (2011), Sun et al. (2009), and Taylor and Fang (2018)). What has not been studied are the consequences of the implicit overlap that arises when assessing risk measures at a higher frequency than the horizon for risk assessment.

If the sampling frequency of the return data is more granular than the horizon for risk assessment, three strategies for estimating and forecasting risk measures are commonly adopted: (a) derive a risk estimate that matches the return interval specified (e.g., one-day volatility from daily return data) and then either use (square-root) scaling or derive model-based multi-step forecasts to obtain estimates for longer (e.g., monthly, annual) horizons; (b) temporally aggregate the underlying data so that they match the horizon for risk assessment, leading to analyses with overlapping samples; or (c) temporally aggregate the data so that samples do not overlap. A detailed analysis and discussion of the tradeoff between sampling frequency and forecast horizon is given in Andersen and Bollerslev (1998) and Andersen et al. (1999). More recently Kole et al. (2017) also studied the impact of temporal and portfolio aggregation on the quality of ten-day ahead value-at-risk (i.e., loss quantile) forecasts.

In the following, we restrict our analysis to the return *variance*, since other risk measures, such as volatility, value-at-risk or expected shortfall, are directly or indirectly related to variance. Moreover, for the sake of simplicity, we assume that returns are recorded at a daily frequency—implying that the most granular sampling and assessment frequency is daily. Note, however, our results also apply to intraday analyses. To better illustrate the estimation strategies (a)–(c), Fig. 1 depicts possible specifications for return interval and data sampling schemes in h-day-ahead assessments. The two rows in each of the three panels indicate the return data used for estimation on day t and $t+1$, respectively. Panel (a) reflects the sampling scheme for risk estimation based on daily return data. In this case, to derive h-day-horizon estimates, one needs to either rely on a scaling rule that approximates h-day risk from one-day estimates or resort to some multi-step forecasting procedure. Panel (b) illustrate the sampling when estimating with overlapping h-day returns at times t and $t+1$. Finally, Panel (c) shows the sampling scheme for returns when estimates are based on non-overlapping return intervals, revealing the implicit overlap when the assessment frequency is higher than the data sampling frequency. It is the latter scheme that is the main focus here.

Frankland et al. (2019) discuss the calibration of value-at-risk models with overlapping data and consider sampling strategies (a)–(c) in the context of Solvency II regulation. They focus on comparing strategy (b) (overlapping returns) with strategy (c) (non-overlapping returns) with regards to the bias and mean squared error when estimating the first four cumulants. They also explore sampling strategies in line with our strategy (a), i.e., the use of non-overlapping data of higher frequency (e.g., monthly) for model estimation in combination with annualization or temporal-aggregation. Moreover, biases arising from the usage of overlapping returns (sampling strategy (b)) when estimating volatilities, variances or other risk measures have been studied in Bod et al. (2002), Kluitman and Franses (2002), Sun et al. (2009), and Taylor and Fang (2018).

Our work differs in two respects: First, we focus directly on strategies based on longer, namely, h-day-return intervals. Given that BCBS (2016, 2019) explicitly rules out any risk assessment based on scaling (but also to avoid excessive clutter), we do not consider scaling strategies. For a discussion of the square-root-of-time scaling see Christoffersen et al. (1998), Daníelsson and Zigrand (2006), Diebold et al. (1997) and McNeil and Frey (2000). Scaling rules under other than multivariate normal processes and, especially, serially dependent observations are also derived in Embrechts et al. (2005). Second, whereas the focus of previous studies has been primarily on the accuracy of risk estimates (i.e., bias, variance, mean squared error etc.) at a given period, our focus is on the dynamic properties of risk estimates.

The choice between (b) (overlapping returns) and (c) (non-overlapping returns) is an ongoing debate among practitioners as well as researchers. The two sampling strategies have, for example, been compared and discussed in the context of insur-

ance regulation (Frankland et al., 2019) and banking regulation (Kontaxis and Tsolas, 2021; 2022). According to Kontaxis and Tsolas (2021, 2022) and Frankland et al. (2019), financial institutions tend to use overlapping returns for estimating risk measures like value-at-risk. One of the main arguments for using overlapping returns is limited data availability. On the other hand, Kontaxis and Tsolas (2021, 2022) argue that non-overlapping returns might be preferable because overlapping returns are, by construction, highly autocorrelated (see Section 3.2). This induced autocorrelation structure can render backtesting procedures invalid. Moreover, it may introduce problems in estimating risk measures and in statistical tests (see Kontaxis and Tsolas (2021, 2022) and Frankland et al. (2019)). Whereas Frankland et al. (2019) conclude that using overlapping returns is preferable for risk estimation, Kontaxis and Tsolas (2021, 2022) recommend using non-overlapping returns.

When assessing variances at a higher frequency (e.g., daily) from non-overlapping return data that have longer return interval (e.g., weekly or monthly returns) we need to be concerned. We show that standard variance estimators, such as the moving-window sample variance or the exponentially-weighted moving average (EWMA) variance estimator (Longerstaey and Spencer, 1996), tend to exhibit strong but spurious sawtooth-type patterns. Risk managers who are obliged to assess risk more often (e.g., daily) than the horizon for risk-assessment implies (e.g., ten days in the Basel III or 259 days in the Solvency II framework) need to be aware that this tends to induce strong spurious seasonal patterns in their risk estimates. We demonstrate this phenomenon both empirically from real data and theoretically for well-behaved data-generating processes (DGPs), such as Gaussian white noise or GARCH(p, q) processes. We derive the theoretical autocorrelation function (ACF) for sequences of successive variance estimates for a broad class of DGPs and variance estimators. Moreover, we present variance estimators, based on overlapping h-day-return intervals, that overcome the problem of spurious seasonality. Our theoretical results are in line with the simulation-based results of Frankland et al. (2019), who, for risk assessment, favor sampling strategy (b) (overlapping returns) combined with bias correction over sampling strategy (c) (non-overlapping returns).

The paper is organized as follows. In Section 2, using real data, we empirically illustrate and explain the presence of spurious seasonality in sequentially estimated variances. Section 3 defines the DGPs considered in this study, summarizes relevant results pertaining to stochastic processes and temporal aggregation, and derives quadratic-form representations for variance estimators. The theoretical ACF for sequences of daily estimated variances is derived in Section 4. Moreover, the phenomenon of spurious seasonality is illustrated and explained on theoretical grounds. Alternative variance estimators based on overlapping return intervals that do not suffer from spurious seasonality are discussed in Section 5. Section 6 summarizes and concludes. All proofs are deferred to Appendix A. Additional results and figures are provided in Appendix B.

2. Spurious Seasonality in Variance Estimates from Temporally Aggregated, Non-Overlapping Returns

We are especially interested in the dynamic properties of sequential variance estimates. To illustrate the issue, we consider bi-weekly returns (i.e., returns over ten trading days) of the Dow Jones Industrial Average (DJIA). Our data source is Williamson (2021). We look at two ways of displaying sequential variance estimates. First, we compute ten different bi-weekly return series, one for each of the ten trading days in the two-week window. For each of the ten return series we derive series of bi-weekly variance estimates, using the EWMA variance estimator (Longerstaey and Spencer, 1996)

$$\sigma^2_{(h),t,\lambda} = \frac{h}{\operatorname{tr}(\mathcal{Q}_{(h),\Delta,\lambda})} \frac{1-\lambda}{1-\lambda^{\Delta}} \sum_{\delta=0}^{\Delta-1} \lambda^{\delta} (r_{(h),t-h\delta} - \mu_{(h),t,\lambda})^2, \tag{2.1}$$

where $r_{(h),t}$ is the h-day return at time t and $\mu_{(h),t,\lambda} = \frac{1-\lambda}{1-\lambda^{\Delta}} \sum_{\delta=0}^{\Delta-1} \lambda^{\delta} r_{(h),t-h\delta}$ is the EWMA estimator for the first moment. The multiplicative constant $\frac{h}{\operatorname{tr}(\mathcal{Q}_{(h),\Delta,\lambda})} = \left(1 - \frac{(1-\lambda)^2(1-\lambda^{2\Delta})}{(1-\lambda^{\Delta})^2(1-\lambda^2)}\right)^{-1}$ is the bias-correction factor, see (3.2). We set $\lambda = 0.96$ and use a moving-window of length $\Delta = 100$. The upper graph in Fig. 2 shows the ten different series of variance estimates, $(\sigma^2_{(10),10t+\tau,\lambda})_{t\in\mathbb{Z}}$, for $1 \le \tau \le 10$, each corresponding to a specific starting day. The lower graph in Fig. 2 is obtained by connecting the ten bi-weekly variance estimates to form a single, daily sequence of estimates. In other words, in the upper graph in Fig. 2 the assessment and sampling frequencies are synchronized and equal to the aggregation horizon of $h = 10$ days. By synchronization of the assessment and sampling frequency we mean that the value of $\tau \in \{1, \ldots, h\}$ is the same for the series of bi-weekly returns, $(r_{(10),10t+\tau,\lambda})_{t\in\mathbb{Z}}$, used for the estimation and the series of bi-weekly variance estimates, $(\sigma^2_{(10),10t+\tau,\lambda})_{t\in\mathbb{Z}}$. That is, both series are sampled on the same equidistant grid where we observe bi-weekly returns and estimate the variance every h-th day. In contrast, the lower graph of Fig. 2 shows the daily sequence of EWMA variance estimates, $(\sigma^2_{(h),t,\lambda})_{t\in\mathbb{Z}}$, based on non-overlapping h-day returns. The distance between two adjacent points of the sequence of variance estimates is always one day rather than ten days, as is the case with the plots in the upper graph. The lower graph is obtained from the upper graph by appropriately joining the bi-weekly estimates, $(\sigma^2_{(10),t,\lambda})_{t\in\mathbb{Z}}$, obtained at a daily frequency and shown in the upper graph. Note that for each specific day t there is exactly one variance estimate $\sigma^2_{(h),t,\lambda}$ giving rise to the daily series shown in the lower graph of Fig. 2 and which is constructed by picking the respective estimate from one of the ten color-coded (color figures can be found in the online version of the article) variance series, each with h-day assessment frequency, shown in the upper graph. Thus, "appropriately joining" means that the lower graph can be obtained from the upper graph by repeatably iterating in the same order through the ten different color-coded series. The first (last) estimates in both graphs are for 01-Jan-2010 (for 31-Dec-2020). The corresponding ten-day log-returns are plotted at the bottom of both graphs with axis on the right.

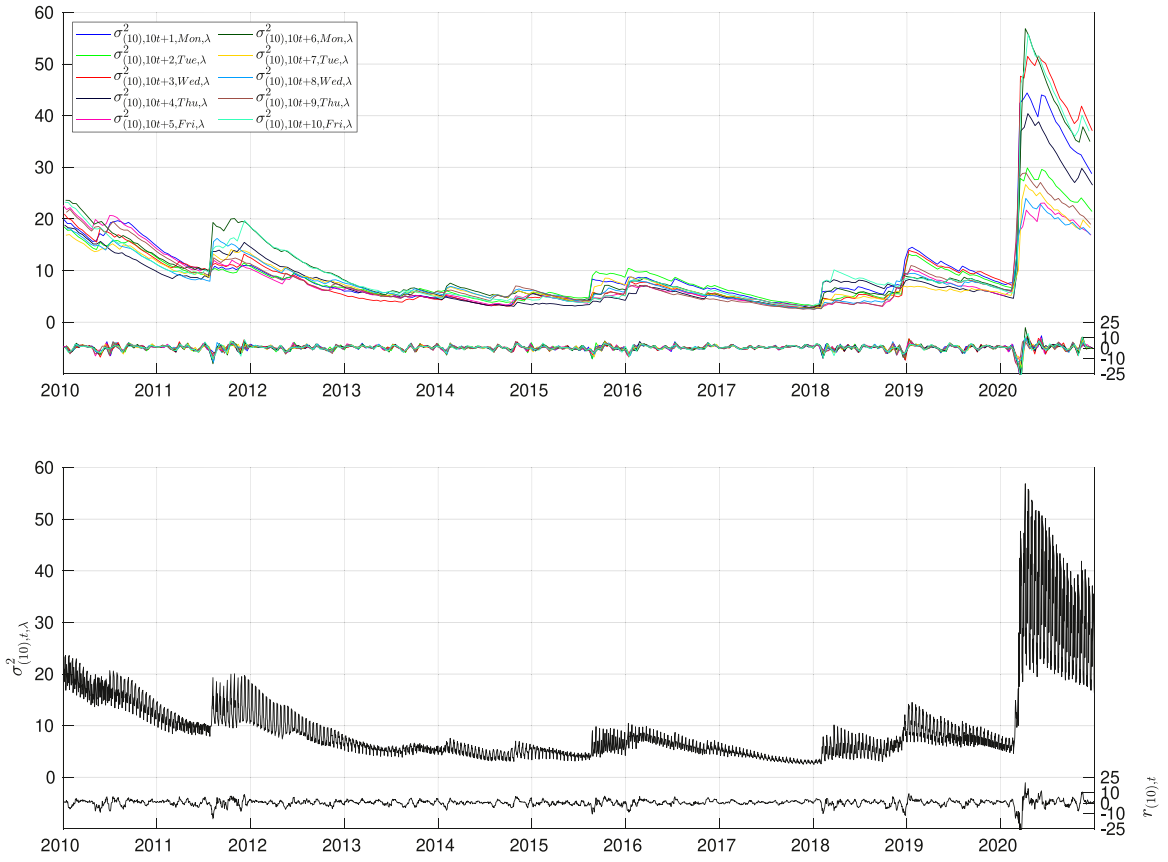

Fig. 2. Estimated EWMA variances of the Dow Jones Industrial Average (DJIA) based on ten-day log-returns with a window length of 100 bi-weekly returns and an EWMA parameter of $\lambda = 0.96$. The first (last) estimates in both graphs are for 01-Jan-2010 (for 31-Dec-2020). The upper graph shows the ten series of bi-weekly variance estimates, each corresponding to a specific weekday and start date, and the lower graph the daily series of bi-weekly variance estimates. The corresponding ten-day log-returns are plotted at the bottom of both graphs with axis on the right.

Each variance estimate shown in Fig. 2 is based on non-overlapping ten-day returns. However, the assessment frequency of the estimates is higher than the sampling frequency of the underlying data set. As a consequence, there is a substantial overlap in data used for successive estimates.

The pronounced sawtooth pattern of the series of daily variance estimates shown in the lower graph of Fig. 2 has direct consequences for the capital requirements of financial institutions. For simplicity, consider a long position in an equity instrument like the DJIA. Under certain conditions (e.g., for Gaussian white noise processes or GARCH processes with normal or Student-t distributed innovations for the returns), risk measures like value-at-risk or expected shortfall are proportional to the (conditional) volatility. This means that series of estimates for these risk measures are prone to exhibit the equivalent sawtooth patterns as the series of variance estimates. These periodic fluctuations in risk estimates lead to corresponding periodic fluctuations in risk capital, for which provision must be made. Also, periodic fluctuations in value-at-risk estimates might require risk mitigation activities and can have an impact on the results of backtests that are commonly employed for validating risk models (see Christoffersen (1998) and Kuester et al. (2006) for an overview on backtesting methods to validate value-at-risk predictions).

In the following, we study the pronounced sawtooth pattern of the series of daily variance estimates shown in the lower graph of Fig. 2. Furthermore, we investigate the reason for the slowly changing patterns in the ten variance series plotted in the upper graph of Fig. 2. To characterize the properties of estimated variance sequences we examine their ACF. The sample ACF of the daily series of estimates, $(\sigma^2_{(10),t,\lambda})_{t\in\mathbb{Z}}$, based on bi-weekly data, shown in Fig. 3, displays a systematic periodic pattern, a feature we refer to as *spurious seasonality*. As will be shown below, this seasonal pattern is due to the sampling scheme for the data used for variance estimation.

3. Prerequisites and Notation

In this section we introduce the two stochastic processes used in the analysis below, establish necessary notation, and briefly summarize relevant results on the temporal aggregation of stochastic processes. Finally, we introduce the (conditional) variance estimators that are the focus of this study.

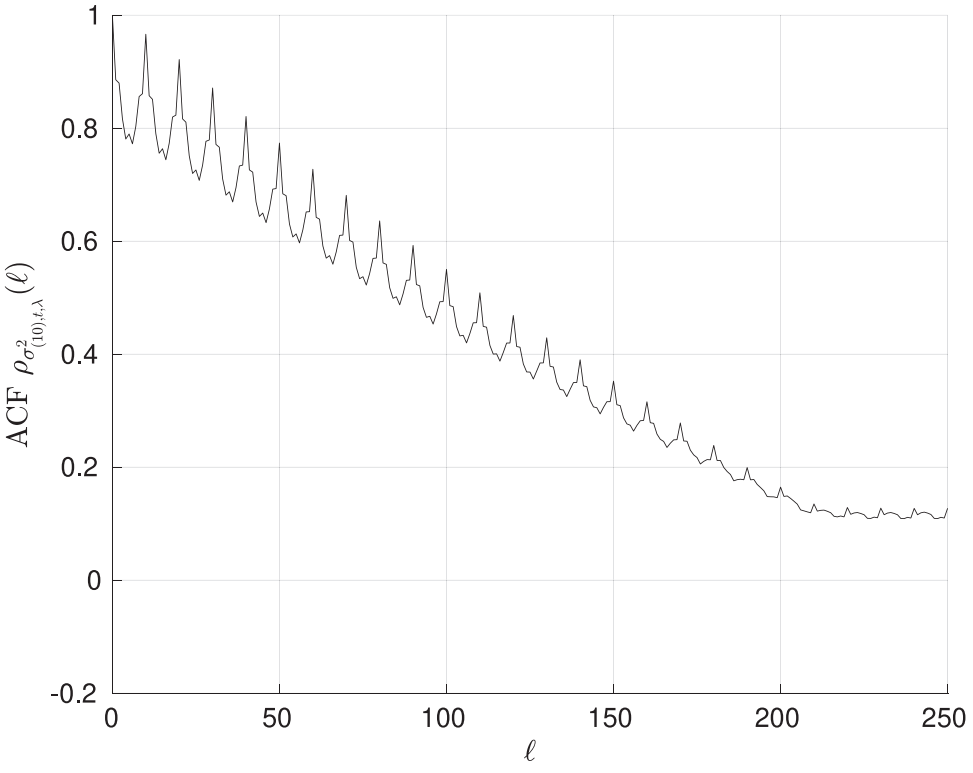

Fig. 3. Sample autocorrelation function (ACF) for the daily series of bi-weekly EWMA variance estimates based on non-overlapping ten-day log-returns. The plot shows the sample ACF for the series of EWMA variance estimates for the Dow Jones Industrial Average (DJIA) from 01-Jan-2010 to 31-Dec-2020.

3.1. Data Generating Stochastic Processes

We consider two DGPs, the Gaussian white noise process and the GARCH(p, q) process. Both processes are so-called weak white noise processes.

Definition 3.1. A stochastic process, $(x_t)_{t\in\mathbb{Z}}$, is called weak white noise process, if $\forall t, t_1, t_2 \in \mathbb{Z}$, $t_1 \neq t_2$:

(i) $E[x_t] = \mu$, with $|\mu| < \infty$,
(ii) $\text{Var}[x_t] = \sigma^2$, with $0 < \sigma^2 < \infty$,
(iii) $\text{Cov}[x_{t_1}, x_{t_2}] = 0$.

The Gaussian white noise process (Example 3.1) is the special case of independent and identically distributed (i.i.d.) random variables with normal distribution.

Example 3.1. A stochastic process, $(x_t)_{t\in\mathbb{Z}}$, is called Gaussian white noise process, if $(x_t)_{t\in\mathbb{Z}}$ is a weak white noise process and $x_t \overset{i.i.d.}{\sim} N(\mu, \sigma^2)$.

As a second case we consider the generalized autoregressive conditional heteroskedasticity (GARCH) process (Example 3.2) introduced by Engle (1982) and Bollerslev (1986), a model class that is widely used both in academic research and in practice in order to model the volatility of financial returns.

Example 3.2. Let $(\varepsilon_t)_{t\in\mathbb{Z}}$ be a sequence of i.i.d. random variables and let $p \in \mathbb{N}$ and $q \in \mathbb{N}_0$. Further, let $\alpha_0 > 0$, $\alpha_1, \ldots, \alpha_q \geq 0$ and $\beta_1, \ldots, \beta_p \geq 0$ and assume $\sum_{i=1}^{q} \alpha_i + \sum_{i=1}^{p} \beta_i < 1$, such that the process is weakly stationary. Then, a GARCH(p, q) process, $(x_t)_{t\in\mathbb{Z}}$, with strictly positive volatility process, $(\sigma_t)_{t\in\mathbb{Z}}$, is defined by

$$x_t = \sigma_t \varepsilon_t, \qquad \sigma_t^2 = \alpha_0 + \sum_{i=1}^{q} \alpha_i x_{t-i}^2 + \sum_{i=1}^{p} \beta_i \sigma_{t-i}^2.$$

The restrictions on the parameter space stated in Example 3.2 guarantee a positive conditional variance σ_t^2 in the case of normally distributed innovations (Bollerslev, 1986). Nelson and Cao (1992) state weaker sufficient conditions for a positive conditional variance which are also necessary (Tsai and Chan, 2008).

3.2. Temporal Aggregation of Returns and Stochastic Processes

Let $(P_t)_{t\in\mathbb{Z}}$ denote the process of daily prices of an asset, $(r_t)_{t\in\mathbb{Z}}$ with $r_t = \ln(P_t) - \ln(P_{t-1})$ the process of daily log-returns, and let vector $\boldsymbol{r}_{t,\delta} := \left[r_{t-\delta+1}, r_{t-\delta+2}, \ldots, r_{t-1}, r_t\right]'$ collect the δ daily returns from day $t-\delta+1$ up to and including day t. h-day returns, $h > 1$, are then given by

$$r_{(h),t} = \ln(P_t) - \ln(P_{t-h}) = \sum_{j=0}^{h-1} r_{t-j} = \mathbf{1}_h' \boldsymbol{r}_{t,h},$$

where $\mathbf{1}_h$ is an $h \times 1$ column vector of ones. We call h the aggregation horizon.

In the following, we will always assume that the process of daily log-returns, $(r_t)_{t\in\mathbb{Z}}$, is generated by a weak white noise process (Definition 3.1) and, in some instances, consider the Gaussian white noise (Example 3.1) and the GARCH(p, q) process (Definition 3.2) as special cases.

If we assume that the daily log-return series, $(r_t)_{t\in\mathbb{Z}}$, is a Gaussian white noise process with $E[r_t] = \mu = 0$ and variance $E[r_t^2] = \sigma^2 < \infty$, the temporally aggregated series, $(r_{(h),th})_{t\in\mathbb{Z}}$, where the sampling frequency coincides with the aggregation horizon, is again a Gaussian white noise process but with variance $E[r_{(h),th}^2] = h\sigma^2 < \infty$. The situation changes, however, when the sampling frequency is lower than the aggregation horizon. This would, for example, be the case when sampling h-day returns, $h > 1$, on a daily basis. Then, $(r_{(h),t})_{t\in\mathbb{Z}}$ turns out to be a non-invertible moving average process of order $h-1$ (in short: MA$(h-1)$ process) (Hansen and Hodrick, 1980), with parameters $\theta_j = 1$ for $1 \le j \le h-1$, i.e., $r_{(h),t} = \sum_{j=0}^{h-1} r_{t-j} = \sum_{j=1}^{h-1} \theta_j r_{t-j} + r_t$, where $(r_t)_{t\in\mathbb{Z}}$ is the weak white noise series of daily log-returns. The theoretical ACF $\rho_{r_{(h),t}}(\ell)$ for the process $(r_{(h),t})_{t\in\mathbb{Z}}$ is given by (cf. Mittnik (1988) or Zinde-Walsh (1988))

$$\rho_{r_{(h),t}}(\ell) = \mathrm{Corr}[r_{(h),t}, r_{(h),t-\ell}] = \begin{cases} \frac{\sum_{j=0}^{h-1-|\ell|}\theta_j\theta_{j+|\ell|}}{\sum_{j=0}^{h-1}\theta_j^2} = \frac{h-|\ell|}{h} & ,\ |\ell| \le h-1, \\ 0 & ,\ |\ell| \ge h, \end{cases}$$

where we set $\theta_0 = 1$ for notational simplicity. Similar results can also be obtained under some regularity conditions for GARCH(p, q) processes. Temporal aggregation of GARCH processes has been investigated by Drost and Nijman (1993), Chan (2022) studies the temporal aggregation of some nonlinear time series processes, and a survey of studies on temporal aggregation of various types of univariate and multivariate time series processes is provided by Silvestrini and Veredas (2008).

3.3. Estimating Variances

Analogous to the vector of daily returns, let $\boldsymbol{r}_{(h),t,\Delta} = [r_{(h),t-h(\Delta-1)}, r_{(h),t-h(\Delta-2)}, \ldots, r_{(h),t-h}, r_{(h),t}]'$ be the Δ-period vector of non-overlapping h-day returns up to and including time t. Denoting the $\Delta \times \Delta$ identity matrix by $\boldsymbol{I}_\Delta$, we define the $h\Delta \times \Delta$ matrix $\boldsymbol{H} = \boldsymbol{I}_\Delta \otimes \mathbf{1}_h$, where $\otimes$ is the Kronecker product, so that $\boldsymbol{r}_{(h),t,\Delta} = \boldsymbol{H}'\boldsymbol{r}_{t,h\Delta}$.

The most common estimator for the dispersion of returns is the sample variance. Defining the idempotent matrix $\boldsymbol{D} \in \mathbb{R}^{\Delta\times\Delta}$, $\boldsymbol{D} = \boldsymbol{I}_\Delta - \frac{1}{\Delta}\mathbf{1}_\Delta\mathbf{1}_\Delta'$, the moving-window sample variance for non-overlapping h-day returns is given by

$$\begin{aligned}\sigma_{(h),t}^2 &= \frac{1}{\Delta-1}\sum_{\delta=0}^{\Delta-1}(r_{(h),t-h\delta} - \mu_{(h),t})^2 = \frac{1}{\Delta-1}\boldsymbol{r}_{(h),t,\Delta}'\boldsymbol{D}'\boldsymbol{D}\boldsymbol{r}_{(h),t,\Delta} \\ &= \frac{1}{\Delta-1}\boldsymbol{r}_{t,h\Delta}'\boldsymbol{H}\boldsymbol{D}\boldsymbol{H}'\boldsymbol{r}_{t,h\Delta},\end{aligned}$$

with $\mu_{(h),t} = \frac{1}{\Delta}\mathbf{1}_\Delta'\boldsymbol{r}_{(h),t,\Delta} = \frac{1}{\Delta}\mathbf{1}_\Delta'\boldsymbol{H}'\boldsymbol{r}_{t,h\Delta}$ being the sample mean.

Below, we only discuss moving-window-type estimators. We restrict ourselves to this kind of estimators because, in practice, estimation is always based on a finite amount of data, so that finite-sample properties are of relevance. The generalization of the results to the increasing-window case is straightforward. Asymptotic properties of sample variances when data are generated by a GARCH process are derived in Horváth et al. (2006).

Many variance estimators can be written as quadratic forms of a vector of daily returns, $\boldsymbol{r}_{t,h\Delta}$, i.e., $\sigma_{(h),t}^2 = \boldsymbol{r}_{t,h\Delta}'\mathcal{Q}\boldsymbol{r}_{t,h\Delta}$, where $\mathcal{Q} \in \mathbb{R}^{h\Delta\times h\Delta}$ is a positive definite, symmetric matrix. Examples are the sample variance given above, but also the exponentially-weighted moving average (EWMA) variance estimator (Longerstaey and Spencer, 1996).

If we assume a weak white noise process (Definition 3.1) for $(r_t)_{t\in\mathbb{Z}}$ with $\mathrm{Var}[r_t] = \sigma^2$, we have $E[\boldsymbol{r}_{t,h\Delta}'\mathcal{Q}\boldsymbol{r}_{t,h\Delta}] = \sigma^2\mathrm{tr}(\mathcal{Q})$, and the bias of the variance estimator, $\boldsymbol{r}_{t,h\Delta}'\mathcal{Q}\boldsymbol{r}_{t,h\Delta}$, is

$$\mathrm{Bias}[\boldsymbol{r}_{t,h\Delta}'\mathcal{Q}\boldsymbol{r}_{t,h\Delta}] = E[\boldsymbol{r}_{t,h\Delta}'\mathcal{Q}\boldsymbol{r}_{t,h\Delta}] - \mathrm{Var}[r_{(h),t}] = \sigma^2(\mathrm{tr}(\mathcal{Q}) - h). \tag{3.1}$$

Therefore, variance estimates of the form $\boldsymbol{r}_{t,h\Delta}'\mathcal{Q}\boldsymbol{r}_{t,h\Delta}$, can be bias-corrected by multiplying with factor $\frac{h}{\mathrm{tr}(\mathcal{Q})}$, i.e., by using

$$\sigma_{(h),t}^2 = \boldsymbol{r}_{t,h\Delta}'\boldsymbol{Q}\boldsymbol{r}_{t,h\Delta} \tag{3.2}$$

as variance estimate with $\boldsymbol{Q} = \frac{h}{\mathrm{tr}(\mathcal{Q})}\mathcal{Q}$. Throughout the paper, we will use the bias-corrected versions of the variance estimators but will, in general, only define $\mathcal{Q}$. Quantities $\boldsymbol{Q}$ and $\mathcal{Q}$ are always related by $\boldsymbol{Q} = \frac{h}{\mathrm{tr}(\mathcal{Q})}\mathcal{Q}$.

Specifically, the sample variance for non-overlapping h-day returns is given by

$$\sigma^2_{(h),t} = \boldsymbol{r}'_{t,h\Delta}\boldsymbol{Q}_{(h),\Delta}\boldsymbol{r}_{t,h\Delta}, \tag{3.3}$$

with $\boldsymbol{\mathcal{Q}}_{(h),\Delta} = \frac{1}{\Delta}\boldsymbol{HDH}' = \frac{1}{\Delta}(\boldsymbol{I}_\Delta \otimes \boldsymbol{1}_h)(\boldsymbol{I}_\Delta - \frac{1}{\Delta}\boldsymbol{1}_\Delta\boldsymbol{1}'_\Delta)(\boldsymbol{I}_\Delta \otimes \boldsymbol{1}'_h)$, and the EWMA variance for non-overlapping h-day returns (2.1) by

$$\sigma^2_{(h),t,\lambda} = \frac{h}{\operatorname{tr}(\boldsymbol{\mathcal{Q}}_{(h),\Delta,\lambda})}\frac{1-\lambda}{1-\lambda^\Delta}\sum_{\delta=0}^{\Delta-1}\lambda^\delta(r_{(h),t-h\delta} - \mu_{(h),t,\lambda})^2 = \boldsymbol{r}'_{t,h\Delta}\boldsymbol{Q}_{(h),\Delta,\lambda}\boldsymbol{r}_{t,h\Delta}, \tag{3.4}$$

with $\boldsymbol{\mathcal{Q}}_{(h),\Delta,\lambda} = \boldsymbol{HE}'\boldsymbol{\Lambda}\boldsymbol{EH}' = (\boldsymbol{I}_\Delta \otimes \boldsymbol{1}_h)(\boldsymbol{I}_\Delta - \boldsymbol{w}\boldsymbol{1}'_\Delta)\boldsymbol{\Lambda}(\boldsymbol{I}_\Delta - \boldsymbol{1}_\Delta\boldsymbol{w}')(\boldsymbol{I}_\Delta \otimes \boldsymbol{1}'_h)$ and $\lambda \in (0,1)$. Vector $\boldsymbol{w} \in \mathbb{R}^{\Delta\times 1}$ and matrices $\boldsymbol{\Lambda}, \boldsymbol{E} \in \mathbb{R}^{\Delta\times\Delta}$ are defined by $\boldsymbol{w} = \frac{1-\lambda}{1-\lambda^\Delta} \times \left[\lambda^{\Delta-1}, \lambda^{\Delta-2}, \ldots, \lambda^1, 1,\right]'$, $\boldsymbol{\Lambda} = \operatorname{Diag}(\boldsymbol{w}) = (\boldsymbol{w}\boldsymbol{1}'_\Delta) \odot \boldsymbol{I}_\Delta$ and $\boldsymbol{E} = \boldsymbol{I}_\Delta - \boldsymbol{1}_\Delta\boldsymbol{w}'$, respectively, with $\odot$ denoting the Hadamard product.

4. Theoretical Autocorrelation of Estimated Variances

4.1. Theoretical Derivation

Let matrices $\boldsymbol{K}, \boldsymbol{L} \in \mathbb{R}^{h\Delta+\ell\times h\Delta}$ be defined by $\boldsymbol{K} = [\boldsymbol{0}_{h\Delta\times\ell}, \boldsymbol{I}_{h\Delta}]'$ and $\boldsymbol{L} = [\boldsymbol{I}_{h\Delta}, \boldsymbol{0}_{h\Delta\times\ell}]'$, $\ell \geq 0$, where $\boldsymbol{0}_{h\Delta\times\ell}$ denotes an $h\Delta \times \ell$ matrix of zeros, so that $\boldsymbol{r}_{t,h\Delta} = \boldsymbol{K}'\boldsymbol{r}_{t,h\Delta+\ell}$ and $\boldsymbol{r}_{t-\ell,h\Delta} = \boldsymbol{L}'\boldsymbol{r}_{t,h\Delta+\ell}$. Variance estimators are then given by the quadratic-form

$$\sigma^2_{(h),t} = \boldsymbol{r}'_{t,h\Delta}\boldsymbol{Q}\boldsymbol{r}_{t,h\Delta} = \boldsymbol{r}'_{t,h\Delta+\ell}\boldsymbol{KQK}'\boldsymbol{r}_{t,h\Delta+\ell}. \tag{4.1}$$

We obtain the sample variance specified in (3.3) for $\boldsymbol{Q} = \boldsymbol{Q}_{(h),\Delta}$ and the EWMA variance specified in (3.4) for $\boldsymbol{Q} = \boldsymbol{Q}_{(h),\Delta,\lambda}$. Similarly, the ($\ell$ days) lagged variance estimator is given by

$$\sigma^2_{(h),t-\ell} = \boldsymbol{r}'_{t-\ell,h\Delta}\boldsymbol{Q}\boldsymbol{r}_{t-\ell,h\Delta} = \boldsymbol{r}'_{t,h\Delta+\ell}\boldsymbol{LQL}'\boldsymbol{r}_{t,h\Delta+\ell}. \tag{4.2}$$

Expressions (4.1) and (4.2) allow us to write the variance estimator, $\sigma^2_{(h),t}$, and its lagged version, $\sigma^2_{(h),t-\ell}$, as quadratic forms of the very same vector of daily returns, $\boldsymbol{r}_{t,h\Delta+\ell}$. The quadratic forms $\boldsymbol{KQK}'$ and $\boldsymbol{LQL}'$ turn out to be block-diagonal matrices, with $\boldsymbol{KQK}' = \operatorname{blkDiag}(\boldsymbol{0}_{\ell\times\ell}, \boldsymbol{Q})$ and $\boldsymbol{LQL}' = \operatorname{blkDiag}(\boldsymbol{Q}, \boldsymbol{0}_{\ell\times\ell})$.

Next, to further analyze the properties of estimated variances based on non-overlapping h-day returns assessed at a frequency higher than the aggregation horizon, we derive the theoretical ACF of the series of estimated variances, $(\sigma^2_{(h),t})_{t\in\mathbb{Z}}$. Theorem 4.1 states a well-known result about the covariance of two quadratic forms of the same multivariate normally distributed random vector. It follows directly from results in Magnus (1978) on moments of products of quadratic forms for multivariate normally distributed random variables.

Theorem 4.1. *Let $\boldsymbol{A}, \boldsymbol{B} \in \mathbb{R}^{n\times n}$ be symmetric matrices and $\boldsymbol{X}$ be a multivariate normally distributed $n \times 1$ vector with $\boldsymbol{\mu} = E[\boldsymbol{X}]$ and $\boldsymbol{\Sigma} = E[(\boldsymbol{X} - \boldsymbol{\mu})(\boldsymbol{X} - \boldsymbol{\mu})'] = E[\boldsymbol{XX}'] - \boldsymbol{\mu}\boldsymbol{\mu}'$. For the quadratic forms $\boldsymbol{X}'\boldsymbol{AX}$ and $\boldsymbol{X}'\boldsymbol{BX}$ we have*

$$\operatorname{Cov}[\boldsymbol{X}'\boldsymbol{AX}, \boldsymbol{X}'\boldsymbol{BX}] = 2\operatorname{tr}(\boldsymbol{A\Sigma B\Sigma}) + 4\boldsymbol{\mu}'\boldsymbol{A\Sigma B\mu}.$$

The following corollary to Theorem 4.1 establishes the theoretical autocovariance function of the variances given by the quadratic forms (3.2) when the daily log-returns, $(r_t)_{t\in\mathbb{Z}}$, follow a Gaussian white noise process. For the sake of simplicity, we assume a Gaussian white noise process with zero mean. In case of $E[r_t] = \mu \neq 0$, we have $\gamma_{\sigma^2_{(h),t}}(\ell) = 2\sigma^4\operatorname{tr}(\boldsymbol{KQK}'\boldsymbol{LQL}') + 4\mu^2\sigma^2\boldsymbol{1}'_{h\Delta+\ell}\boldsymbol{KQK}'\boldsymbol{LQL}'\boldsymbol{1}_{h\Delta+\ell}$.

Corollary 4.1. *Let $(r_t)_{t\in\mathbb{Z}}$ be a Gaussian white noise process (Example 3.1) with $E[r_t] = 0$ and variance $\operatorname{Var}[r_t] = \sigma^2$ and consider variance estimates of the form $\sigma^2_{(h),t} = \boldsymbol{r}'_{t,h\Delta}\boldsymbol{Q}\boldsymbol{r}_{t,h\Delta}$ (Eq. (3.2)). Then, the theoretical autocovariance of the series $(\sigma^2_{(h),t})_{t\in\mathbb{Z}}$, for $\ell \geq 0$, is given by*

$$\gamma_{\sigma^2_{(h),t}}(\ell) = \operatorname{Cov}[\sigma^2_{(h),t}, \sigma^2_{(h),t-\ell}] = 2\sigma^4\operatorname{tr}(\boldsymbol{KQK}'\boldsymbol{LQL}').$$

Note that for $\ell > h\Delta$

$$\gamma_{\sigma^2_{(h),t}}(\ell) = 2\sigma^4\operatorname{tr}(\boldsymbol{KQK}'\boldsymbol{LQL}') = 2\sigma^4\operatorname{tr}(\boldsymbol{0}_{h\Delta\times h\Delta}\,\boldsymbol{Q}\,\boldsymbol{0}_{h\Delta\times h\Delta}\,\boldsymbol{Q}) = 0,$$

and, by definition, the theoretical ACF for $\ell \geq 0$ is given by $\rho_{\sigma^2_{(h),t}}(\ell) = \gamma_{\sigma^2_{(h),t}}(\ell)/\gamma_{\sigma^2_{(h),t}}(0)$.

In the following, we extend Theorem 4.1 to a more general class of weak white noise processes which contains many zero-mean weak white noise processes—especially, the Gaussian white noise process with $\mu = 0$ and GARCH(p, q) processes.

Theorem 4.2. *Let $(x_t)_{t\in\mathbb{Z}}$ be a stochastic process with $E[|x_t|^i]<\infty$, for $t\in\mathbb{Z}$ and $i\leq 4$. For $t_1,t_2,t_3,t_4\in\mathbb{Z}$ with $\forall i,j\in\{t_1,t_2,t_3,t_4\}$, $i\neq j$, we assume*

$$E[x_{t_1}]=0, \tag{4.3}$$

$$E[x_{t_1}x_{t_2}x_{t_3}x_{t_4}]=0, \tag{4.4}$$

$$E[x_{t_1}^3x_{t_2}]=0, \tag{4.5}$$

$$E[x_{t_1}^2x_{t_2}x_{t_3}]=0. \tag{4.6}$$

Let $\boldsymbol{X}=[x_1,\dots,x_n]'$ and define $\boldsymbol{X}^{2\odot}=\boldsymbol{X}\odot\boldsymbol{X}=[x_1^2,\dots,x_n^2]'$. Furthermore, define vector $\boldsymbol{\mu}_{\boldsymbol{X}^{2\odot}}\in\mathbb{R}^{n\times 1}$ and matrices $\boldsymbol{\Sigma}_{\boldsymbol{X}},\boldsymbol{\Sigma}_{\boldsymbol{X}^{2\odot}}\in\mathbb{R}^{n\times n}$ by

$$\boldsymbol{\Sigma}_{\boldsymbol{X}}=E[\boldsymbol{X}\boldsymbol{X}'],\quad \boldsymbol{\mu}_{\boldsymbol{X}^{2\odot}}=E[\boldsymbol{X}^{2\odot}]\quad\text{and}\quad \boldsymbol{\Sigma}_{\boldsymbol{X}^{2\odot}}=E[\boldsymbol{X}^{2\odot}\boldsymbol{X}^{2\odot\prime}]-\boldsymbol{\mu}_{\boldsymbol{X}^{2\odot}}\boldsymbol{\mu}_{\boldsymbol{X}^{2\odot}}',$$

respectively. Then, for symmetric matrices $\boldsymbol{A},\boldsymbol{B}\in\mathbb{R}^{n\times n}$, we have

$$\operatorname{Cov}[\boldsymbol{X}'\boldsymbol{A}\boldsymbol{X},\boldsymbol{X}'\boldsymbol{B}\boldsymbol{X}]=\operatorname{tr}(\boldsymbol{C}(\boldsymbol{\Sigma}_{\boldsymbol{X}^{2\odot}}+\boldsymbol{\mu}_{\boldsymbol{X}^{2\odot}}\boldsymbol{\mu}_{\boldsymbol{X}^{2\odot}}'))-\operatorname{tr}(\boldsymbol{A}\boldsymbol{\Sigma}_{\boldsymbol{X}})\operatorname{tr}(\boldsymbol{B}\boldsymbol{\Sigma}_{\boldsymbol{X}}),$$

where $\boldsymbol{C}=\boldsymbol{a}\boldsymbol{b}'+2\boldsymbol{A}\odot\boldsymbol{B}\odot(\mathbf{1}_n\mathbf{1}_n'-\boldsymbol{I}_n)$, with $\boldsymbol{a}=\operatorname{diag}(\boldsymbol{A})=(\boldsymbol{A}\odot\boldsymbol{I}_n)\mathbf{1}_n$ and $\boldsymbol{b}=\operatorname{diag}(\boldsymbol{B})=(\boldsymbol{B}\odot\boldsymbol{I}_n)\mathbf{1}_n$.

Again, a corollary to Theorem 4.2 establishes the theoretical autocovariance function of the quadratic-form variance estimator when the daily log-return process, $(r_t)_{t\in\mathbb{Z}}$, is a weak white noise process (Definition 3.1) satisfying the moment conditions (4.3)-(4.6).

Corollary 4.2. *Let $(r_t)_{t\in\mathbb{Z}}$ be a weak white noise process fulfilling the moment conditions (4.3)-(4.6). Moreover, let $\sigma^2=\operatorname{Var}[r_t]=E[r_t^2]$ and $\boldsymbol{r}_{t,h\Delta+\ell}^{2\odot}=\boldsymbol{r}_{t,h\Delta+\ell}\odot\boldsymbol{r}_{t,h\Delta+\ell}$, and define vector $\boldsymbol{\mu}_{\boldsymbol{r}_{t,h\Delta+\ell}^{2\odot}}\in\mathbb{R}^{h\Delta+\ell\times 1}$ and matrix $\boldsymbol{\Sigma}_{\boldsymbol{r}_{t,h\Delta+\ell}^{2\odot}}\in\mathbb{R}^{h\Delta+\ell\times h\Delta+\ell}$ by*

$$\boldsymbol{\mu}_{\boldsymbol{r}_{t,h\Delta+\ell}^{2\odot}}=E[\boldsymbol{r}_{t,h\Delta+\ell}^{2\odot}]\qquad\text{and}\qquad \boldsymbol{\Sigma}_{\boldsymbol{r}_{t,h\Delta+\ell}^{2\odot}}=E[\boldsymbol{r}_{t,h\Delta+\ell}^{2\odot}\boldsymbol{r}_{t,h\Delta+\ell}^{2\odot\prime}]-\boldsymbol{\mu}_{\boldsymbol{r}_{t,h\Delta+\ell}^{2\odot}}\boldsymbol{\mu}_{\boldsymbol{r}_{t,h\Delta+\ell}^{2\odot}}',$$

respectively. Then, considering variance estimates of the form $\sigma_{(h),t}^2=\boldsymbol{r}_{t,h\Delta}'\boldsymbol{Q}\boldsymbol{r}_{t,h\Delta}$, the theoretical autocovariance of the series $(\sigma_{(h),t}^2)_{t\in\mathbb{Z}}$, for $\ell\geq 0$, is given by

$$\gamma_{\sigma_{(h),t}^2}(\ell)=\operatorname{tr}\left(\boldsymbol{C}\boldsymbol{\Sigma}_{\boldsymbol{r}_{t,h\Delta+\ell}^{2\odot}}\right)+2\sigma^4\left(\operatorname{tr}(\boldsymbol{K}\boldsymbol{Q}\boldsymbol{K}'\boldsymbol{L}\boldsymbol{Q}\boldsymbol{L}')-\boldsymbol{a}'\boldsymbol{b}\right),$$

with $\boldsymbol{C}=\boldsymbol{a}\boldsymbol{b}'+2(\boldsymbol{K}\boldsymbol{Q}\boldsymbol{K}')\odot(\boldsymbol{L}\boldsymbol{Q}\boldsymbol{L}')\odot(\mathbf{1}_{h\Delta+\ell}\mathbf{1}_{h\Delta+\ell}'-\boldsymbol{I}_{h\Delta+\ell})$, where $\boldsymbol{a}=\operatorname{diag}(\boldsymbol{K}\boldsymbol{Q}\boldsymbol{K}')$ and $\boldsymbol{b}=\operatorname{diag}(\boldsymbol{L}\boldsymbol{Q}\boldsymbol{L}')$.

Remark 4.1. The following processes satisfy the conditions of Corollary 4.2 and especially the moment conditions (4.3)-(4.6):

(i) For $\mu=0$, the Gaussian white noise process (Example 3.1) clearly fulfills all conditions.
(ii) Let $(x_t)_{t\in\mathbb{Z}}$ be a GARCH(p,q) process as defined in Example 3.2. For the innovations, $(\varepsilon_t)_{t\in\mathbb{Z}}$, we assume a sequence of i.i.d. random variables being symmetrically distributed such that odd moments are zero. We further assume that the first four moments of $(x_t)_{t\in\mathbb{Z}}$ exist (conditions for the existence of moments can be found in He and Teräsvirta (1999b) and Bollerslev (1986) for the GARCH(1,1) case and in Ling and McAleer (2002a) for the GARCH(p,q) process). Our Appendix B.1 shows that under these conditions the GARCH(p,q) satisfies all conditions such that Corollary 4.2 holds.
(iii) Due to the moment conditions (4.3)-(4.6), the theoretical autocovariance in Corollary 4.2 only depends on the variance $\sigma^2=\operatorname{Var}[r_t]$, $\boldsymbol{\mu}_{\boldsymbol{r}_{t,h\Delta+\ell}^{2\odot}}$, and the variance-covariance matrix of the vector of squares, $\boldsymbol{\Sigma}_{\boldsymbol{r}_{t,h\Delta+\ell}^{2\odot}}$. If the daily returns are, for example, asymmetrically distributed or follow a GARCH process with leverage, the moment conditions have to be weakened and additional terms, like unconditional skewness, are necessary to compute theoretical autocovariances. Note that these moments are often not available in closed form (He et al., 2008).
(iv) Moment conditions (4.3)-(4.5) can be verified for general classes of GARCH processes $x_t=\sigma_t\varepsilon_t$ under the assumption of zero-mean symmetrically distributed i.i.d. innovations and the existence of the first four moments. However, moment condition (4.6) needs to be verified specifically for each type of GARCH process and, in case (4.6) does not hold, a suitable generalization of Theorem 4.2 would be required. For discussions on families of GARCH processes and conditions on stationarity and the existence of moments see He and Teräsvirta (1999b) and Ling and McAleer (2002b).

The functional form of the relevant unconditional moments for different GARCH processes have been derived in He and Teräsvirta (1999a) and Karanasos (1999).

4.2. Illustration

We illustrate the theoretical results of the previous section by presenting plots of the theoretical ACF and those obtained from a simulation study. All illustrations in this section are for a GARCH(1,1) DGP and the EWMA variance estimator (3.4). Appendix B.2 presents plots for a Gaussian white noise data generating process and variance being estimated by the sample variance (3.3).

Let $(r_t)_{t\in\mathbb{Z}}$ be generated by the GARCH(1,1) process

$$r_t = \sigma_t \varepsilon_t, \quad \sigma_t^2 = \alpha_0 + \alpha_1 r_{t-1}^2 + \beta_1 \sigma_{t-1}^2, \tag{4.7}$$

with $\varepsilon_t \overset{i.i.d.}{\sim} \mathcal{N}(0,1)$ and parameter vector, $[\alpha_0, \alpha_1, \beta_1]' = [0.01, 0.05, 0.94]'$, parameter values that are typical for daily stock returns. As estimator for the h-day variance at time t we use the EWMA estimator (3.4) with $\lambda = 0.96$. In view of the Basel III rules (BCBS, 2016), we chose $h = 10$ as aggregation horizon, i.e., we consider a bi-weekly target horizon as, for example, in Kole et al. (2017).

As for the ten-day return series itself, we can obtain ten different series of estimates for the variance if we synchronize assessment and sampling frequencies to be equal to the aggregation horizon of $h = 10$ days, namely, $(\sigma^2_{(h),ht+\tau,\lambda})_{t\in\mathbb{Z}}$, for $1 \le \tau \le h$. By synchronization of the assessment and sampling frequency we mean that the value of $\tau \in \{1, \dots, h\}$ is the same for the series of h-day returns, $(r_{(h),ht+\tau,\lambda})_{t\in\mathbb{Z}}$, and the series of (assessed) variance estimates, $(\sigma^2_{(h),ht+\tau,\lambda})_{t\in\mathbb{Z}}$. That is, both series are sampled on the same equidistant grid where we observe h-day returns and estimate the variance every h-th day. As window length for the rolling-window estimates we choose $\Delta = 100$, giving rise to $h\Delta = 1000$ daily observations which corresponds to roughly four years of return data. At any point in time, each estimate is based on Δ non-overlapping h-day returns or $h\Delta$ daily returns. Two consecutive estimates, $\sigma^2_{(h),t,\lambda}$ and $\sigma^2_{(h),t+1,\lambda}$ (or $\sigma^2_{(h),t-1,\lambda}$), have $h\Delta - 2$ daily return observations in common. We simulate GARCH(1,1) process (4.7) with a sample size of 2000 trading days, about eight calendar years.

The upper graph in Fig. 4 shows the ten different series of variance estimates, $(\sigma^2_{(h),th+\tau,\lambda})_{t\in\mathbb{Z}}$, $1 \le \tau \le h$, obtained when assessment and sampling frequencies are synchronized. In each of the ten plots, two adjacent points of the series, $(\sigma^2_{(h),th+\tau,\lambda})_{t\in\mathbb{Z}}$, $1 \le \tau \le h$, have distance $h = 10$. The lower graph shows the sequence of daily EWMA variance estimates, $(\sigma^2_{(h),t,\lambda})_{t\in\mathbb{Z}}$, based on non-overlapping h-day returns.

The plots for the simulations in Fig. 4 are constructed as those for the DJIA returns in Fig. 2. The daily series of EWMA variance estimates (lower graph in Fig. 4) fluctuates in a highly regular fashion, mimicking a strong seasonal pattern. Clearly, from a risk management perspective, such strong fluctuations are bound to have detrimental implications as they induce volatile risk capital charges and risk mitigation activities.

To derive the theoretical autocovariances of the series of variance estimates, $(\sigma^2_{(h),t,\lambda})_{t\in\mathbb{Z}}$, assuming a GARCH(1,1) process for the daily returns, $(r_t)_{t\in\mathbb{Z}}$, we use the fact that the variance-covariance matrix of the vector of squared returns, $\boldsymbol{r}^{2\odot}_{t,h\Delta+\ell} = [r^2_{t-h\Delta-\ell+1}, \dots, r^2_t]'$, is given by the symmetric Toeplitz matrix (cf. He and Teräsvirta (1999a) or Karanasos (1999))

$$\boldsymbol{\Sigma}_{\boldsymbol{r}^{2\odot}_{t,h\Delta+\ell},[i,i+j]} = \begin{cases} \gamma_{r_t^2}(0), & 1 \le i \le h\Delta+\ell,\ j = 0, \\ \frac{\gamma_{r_t^2}(1)}{(\alpha_1+\beta_1)^{1-j}}, & 1 \le i \le h\Delta+\ell-1,\ 1 \le j \le h\Delta+\ell-i, \end{cases}$$

where $\gamma_{r_t^2}(0)$ and $\gamma_{r_t^2}(1)$ denote the variance and theoretical first-order autocovariance, respectively, of the squared returns from a GARCH(1,1) process. Thus, if daily returns follow a GARCH(1,1) process, the theoretical autocorrelation of the process of daily exponentially-weighted moving-average variances (3.4), $(\sigma^2_{(h),t,\lambda})_{t\in\mathbb{Z}}$, based on non-overlapping h-day returns, can be computed via Corollary 4.2 by plugging in $\mathbf{Q}_{(h),\Delta,\lambda}$, $\boldsymbol{\Sigma}_{\boldsymbol{r}^{2\odot}_{t,h\Delta+\ell}}$ and $\mathrm{Var}(r_t) = \alpha_0/(1-\alpha_1-\beta_1)$ into the formula for the theoretical autocovariance and scaling via $\rho_{\sigma^2_{(h),t,\lambda}}(\ell) = \gamma_{\sigma^2_{(h),t,\lambda}}(\ell)/\gamma_{\sigma^2_{(h),t,\lambda}}(0)$.

The theoretical ACF with estimates based on daily return samples of size $h\Delta = 1000$ is presented on the left in Fig. 5. The graph shows the effect for the aggregation horizons $h = 5, 10, 20$, amounting to quasi-weekly, quasi-bi-weekly and quasi-monthly return periods. It demonstrates that the theoretical ACF of EWMA variances, $\rho_{\sigma^2_{(h),t,\lambda}}(\ell)$, based on non-overlapping h-day returns, is highly cyclical and slowly decaying. The (spurious) seasonality that is present in the sample ACF of estimated variances for the DJIA data (Fig. 3) is compatible with the (spurious) seasonality in the theoretical ACF in Fig. 5. The right graph in Fig. 5 further illustrates the interaction between aggregation horizon, h, and the window length, Δ. The aggregation horizon is bi-weekly ($h = 10$) and the window length, Δ, assumes values 25, 50 and 100, i.e., roughly one, two and four calendar years of daily returns, respectively.

Although the formula for the theoretical autocovariance $\gamma_{\sigma^2_{(h),t,\lambda}}(\ell)$ in Corollary 4.2 turns out to be useful, it offers little insight into where the spurious seasonality exactly comes from or how the amplitude of the periodic spurious seasonality in the theoretical ACF depends on the variance estimator or the DGP. Appendix B.3 expresses the theoretical ACF as the sum of three components, which provide more insight and show that the term $(\boldsymbol{KQK}') \odot (\boldsymbol{LQL}')$ is crucially responsible for the spurious seasonality in the theoretical ACF.

The upper graph in Fig. 4 shows a pronounced periodicity, though it is not always the same observation within the h-day periods that assumes the highest or lowest value. In other words, the order statistics of the different estimates within

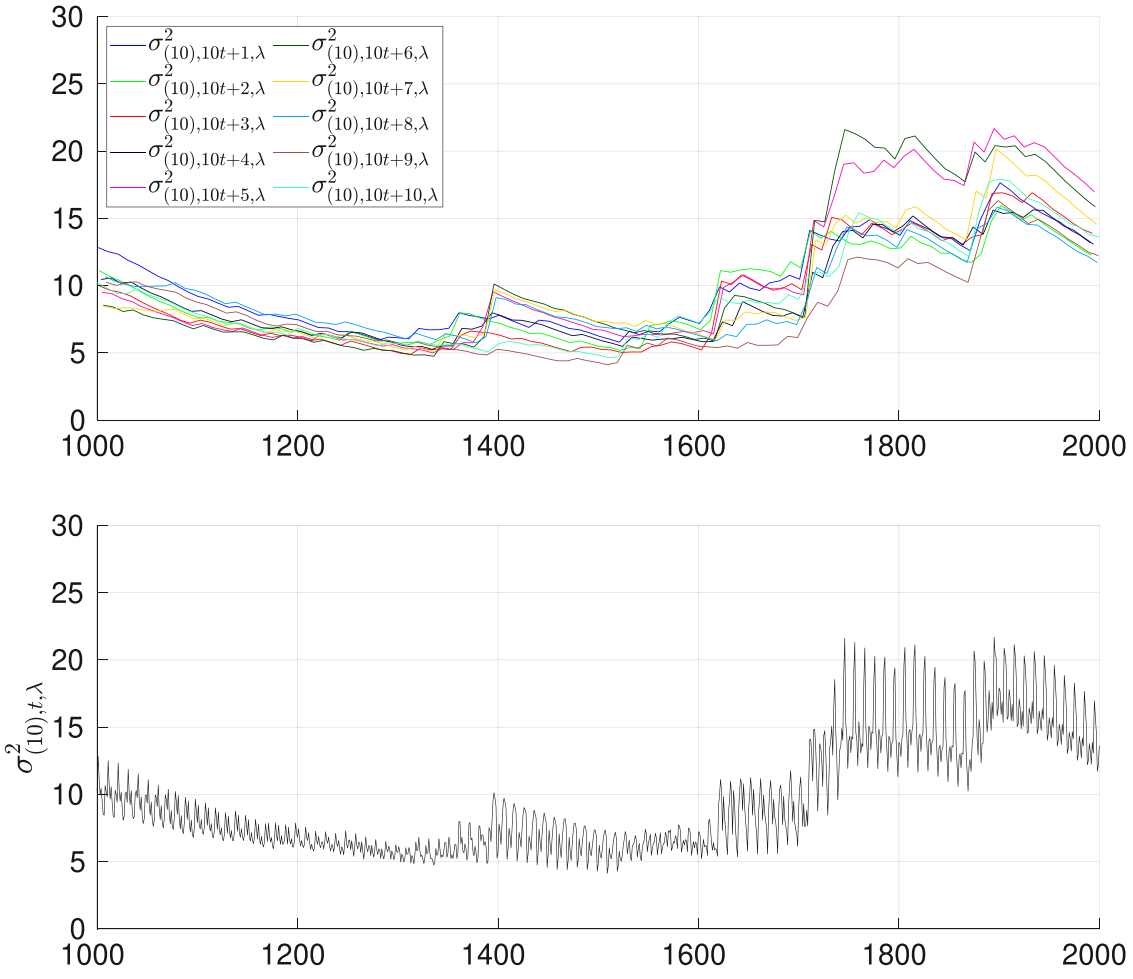

Fig. 4. Time series of EWMA variance estimates (3.4), $\sigma^2_{(h),t,\lambda}$, for simulated daily return series from GARCH(1,1) process (4.7). The upper plot shows the estimates $(\sigma^2_{(10),10t+\tau,\lambda})_{t\in\mathbb{Z}}$, for $1 \le \tau \le 10$. The lower plot shows the series $(\sigma^2_{(10),t,\lambda})_{t\in\mathbb{Z}}$. Both plots are based on bi-weekly ($h = 10$) returns and estimation window $\Delta = 100$.

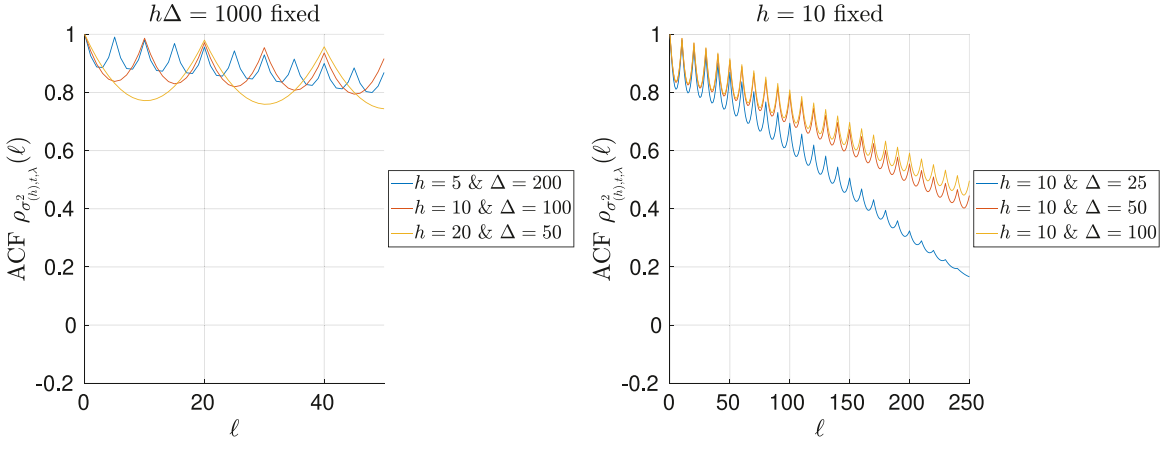

Fig. 5. The ACF of EWMA variances (3.4), $\sigma^2_{(h),t,\lambda}$, for daily returns from GARCH(1,1) process (4.7). For the left plot we use a fixed number of daily returns to derive the EWMA variances. The right plot depicts the ACF of EWMA variances based on bi-weekly ($h = 10$) returns and estimation windows $\Delta = 25, 50, 100$.

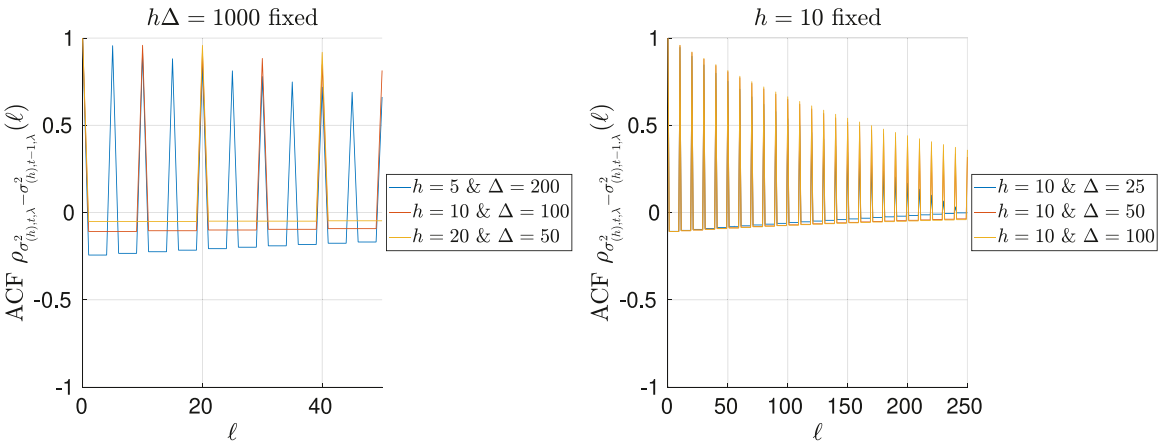

Fig. 6. The ACF of the first difference of EWMA variances (3.4), $\sigma^2_{(h),t,\lambda}$, for daily returns from GARCH(1,1) process (4.7). For the left plot we use a fixed number of daily returns to derive the EWMA variances. The right plot depicts the ACF of the first difference of EWMA variances based on bi-weekly ($h = 10$) returns and estimation windows $\Delta = 25, 50, 100$.

an h-day period fluctuate, but do so rather slowly. Therefore, if the focus is on bi-weekly risk estimation but assessment occurs at a daily frequency, then, by construction, the ordering of the ten different variance estimates in a two-week period gradually changes over time. The color-coded series of EWMA variances in the upper graph of Fig. 4 make clear that, at some point in time, any particular color may be on top (or bottom) and that there is a high probability that this will also hold for the following h-day period.

To get further insights into why the order statistics gradually change over time, we take a look at the theoretical autocovariance of the first difference of the estimated variances,

$$\gamma_{\sigma^2_{(h),t}-\sigma^2_{(h),t-1}}(\ell) = 2\gamma_{\sigma^2_{(h),t}}(\ell) - \gamma_{\sigma^2_{(h),t}}(\ell+1) - \gamma_{\sigma^2_{(h),t}}(|\ell-1|), \quad \ell \geq 0.$$

The theoretical ACF of the first differences of the estimated variances, $\rho_{\sigma^2_{(h),t,\lambda}-\sigma^2_{(h),t-1,\lambda}}(\ell)$, is plotted in Fig. 6, where we used the same settings as for the theoretical ACF of the EWMA variances shown in Fig. 5.

The plots in Fig. 6 demonstrate that the series of first differences is highly autocorrelated for lags being multiples of the aggregation horizon, h. This means, the change of the estimate from one day to another is highly autocorrelated with that of h days ago. At lags that are not multiples of h, the autocorrelations of the first-order differences are quite small and slightly negative. This behavior explains the slowly changing ordering of the h different variance series in the upper graph of Fig. 4.

5. The Case of Overlapping Aggregated Returns

The previous section showed that daily variance estimates based on non-overlapping h-day returns exhibit spurious seasonality. In cases where the aggregation horizon is fixed, the only alternative is to synchronize both assessment and sampling at a daily frequency, i.e., to use overlapping h-day returns for daily risk estimations. In the following we consider variance estimators for overlapping returns that avoid spurious seasonality.

The simplest variance estimator based on overlapping h-day returns is to apply standard formulas for variance estimators to sets of overlapping return observations. The quadratic-form representation for the sample variance for overlapping h-day returns is given by

$$\breve{\sigma}^2_{(h),t} = \frac{h}{\mathrm{tr}(\breve{\boldsymbol{Q}}_{(h),\Delta})} \frac{1}{h(\Delta-1)+1} \sum_{\tau=0}^{h(\Delta-1)} (r_{(h),t-\tau} - \breve{\mu}_{(h),t})^2 = \boldsymbol{r}'_{t,h\Delta} \breve{\boldsymbol{Q}}_{(h),\Delta} \boldsymbol{r}_{t,h\Delta}, \tag{5.1}$$

with $\breve{\boldsymbol{Q}}_{(h),\Delta} = \frac{1}{h(\Delta-1)+1} \sum_{j=0}^{h-1} \boldsymbol{S}'_j \boldsymbol{S}_j$, $\boldsymbol{S}_0 = \boldsymbol{H}' - \boldsymbol{1}_\Delta \boldsymbol{1}'_\Delta \boldsymbol{J}'$, $\boldsymbol{H} = \boldsymbol{I}_\Delta \otimes \boldsymbol{1}_h$ and $\boldsymbol{S}_j = \boldsymbol{H}'_j - \boldsymbol{a}\boldsymbol{1}'_\Delta \boldsymbol{J}'$, for $1 \leq j \leq h-1$, where $\boldsymbol{J} = \boldsymbol{H} + \sum_{j=1}^{h-1} \boldsymbol{H}_j$, $\boldsymbol{a} = \begin{bmatrix} \boldsymbol{1}'_{\Delta-1} & 0 \end{bmatrix}'$ and

$$\boldsymbol{H}_j = \begin{bmatrix} \boldsymbol{0}_{h-j} & \boldsymbol{0}_{(h-j)\times(\Delta-1)} \\ \boldsymbol{0}_{h(\Delta-1)} & \boldsymbol{I}_{\Delta-1} \otimes \boldsymbol{1}_h \\ \boldsymbol{0}_j & \boldsymbol{0}_{j\times(\Delta-1)} \end{bmatrix},$$

where $\boldsymbol{0}_n$ is a column vector with n zeros and $\boldsymbol{0}_{n\times m}$ denotes a $n \times m$ matrix of zeros. The EWMA variance for overlapping h-day returns is given by

$$\breve{\sigma}^2_{(h),t,\lambda} = \frac{h}{\mathrm{tr}(\breve{\boldsymbol{Q}}_{(h),\Delta,\lambda})} \frac{1-\lambda^{\frac{1}{h}}}{1-\lambda^{\frac{h(\Delta-1)+1}{h}}} \sum_{\tau=0}^{h(\Delta-1)} \lambda^{\frac{\tau}{h}} (r_{(h),t-\tau} - \breve{\mu}_{(h),t,\lambda})^2 = \boldsymbol{r}'_{t,h\Delta} \breve{\boldsymbol{Q}}_{(h),\Delta,\lambda} \boldsymbol{r}_{t,h\Delta}, \tag{5.2}$$

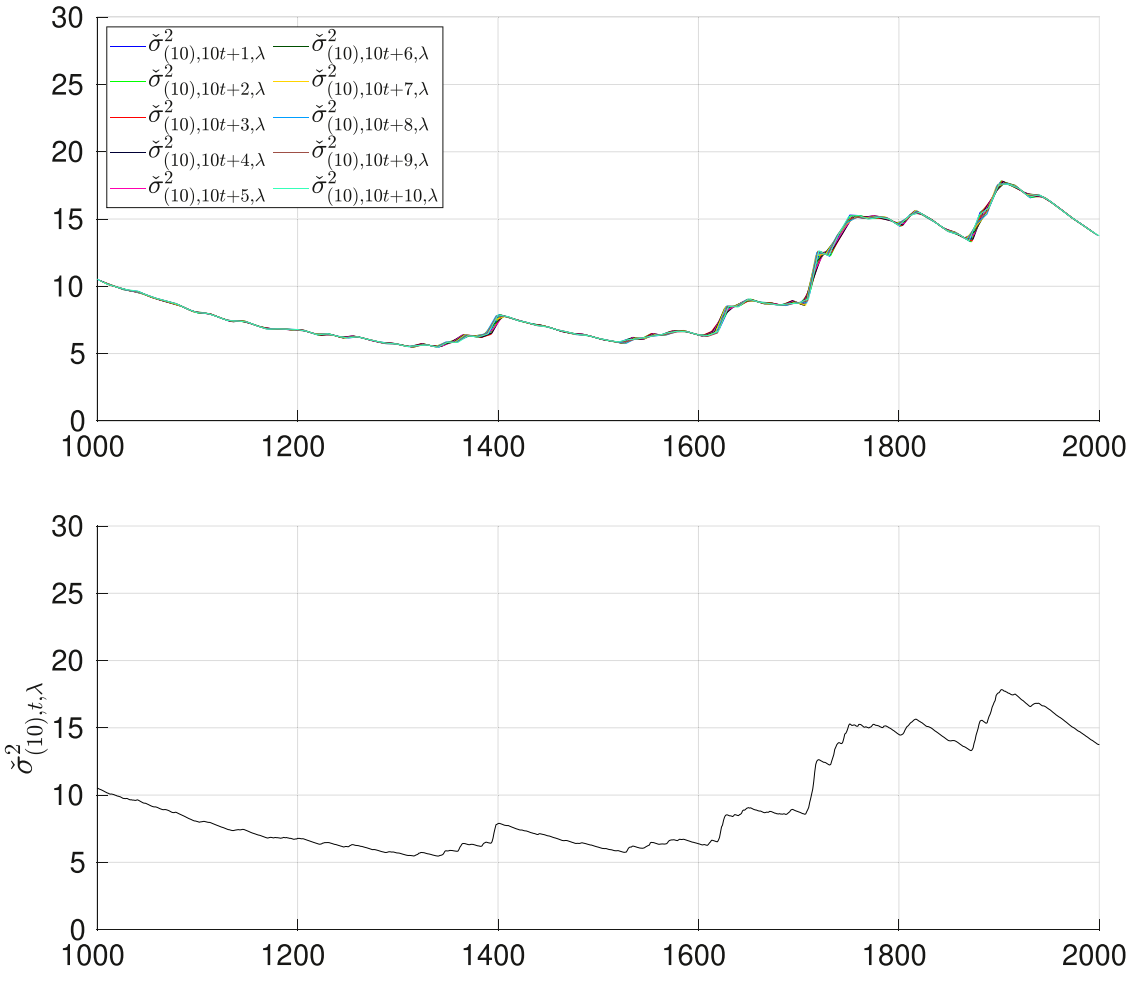

Fig. 7. Time series of EWMA variance estimates with overlapping data (5.2), $\check{\sigma}^2_{(h),t,\lambda}$, for simulated daily return series from GARCH(1,1) process (4.7). The upper plot shows the estimates $(\check{\sigma}^2_{(10),10t+\tau,\lambda})_{t\in\mathbb{Z}}$, for $1 \le \tau \le 10$. The lower plot shows the series $(\check{\sigma}^2_{(10),t,\lambda})_{t\in\mathbb{Z}}$. Both plots are based on bi-weekly ($h = 10$) returns and estimation window $\Delta = 100$.

with $\check{\mathcal{Q}}_{(h),\Delta,\lambda} = \sum_{j=0}^{h-1} \lambda^{\frac{j}{h}} \tilde{\boldsymbol{S}}_j' \boldsymbol{\Gamma} \tilde{\boldsymbol{S}}_j$, $\tilde{\boldsymbol{S}}_0 = \boldsymbol{H}' - \mathbf{1}_\Delta \boldsymbol{\gamma}' \boldsymbol{G}'$ and $\tilde{\boldsymbol{S}}_j = \boldsymbol{H}_j' - \boldsymbol{a}\boldsymbol{\gamma}' \boldsymbol{G}'$, for $1 \le j \le h-1$, with $\boldsymbol{G} = \boldsymbol{H} + \sum_{j=1}^{h-1} \lambda^{\frac{j}{h}} \boldsymbol{H}_j$ and, for $\lambda \in (0,1)$, $\boldsymbol{\Gamma} = \mathrm{Diag}(\boldsymbol{\gamma}) = (\boldsymbol{\gamma}\mathbf{1}_\Delta') \odot \boldsymbol{I}_\Delta$, where $\boldsymbol{\gamma} = \frac{1-\lambda^{1/h}}{1-\lambda^{(h(\Delta-1)+1)/h}} \left[\lambda^{\Delta-1}, \lambda^{\Delta-2}, \ldots, \lambda^1, 1, \right]'$.

If we apply the EWMA variance estimator for overlapping returns (5.2) to the same simulated GARCH(1,1) series underlying Fig. 4, we obtain the series of variance estimators plotted in Fig. 7. The lower graph in Fig. 7 clearly shows the absence of spurious seasonality as compared to the lower graph in Fig. 4. The ten different series of variance estimates (upper graph in Fig. 7), where assessment and sampling frequencies are in sync and equal to the aggregation horizon, h, turn out to be much more stable; and long-memory effects in the order statistics, associated with h-day periods, are no longer present.

Note that the theoretical autocovariances for the daily EWMA variance estimates for overlapping returns can again be obtained from Corollary 4.2. The corresponding theoretical ACF of the estimated variances is shown in Fig. 8. The DGP and the combinations of aggregation horizons, h, and estimation window length, Δ, are the same as in Fig. 5. The periodicity in the theoretical ACF has been eliminated, and the functional form of the theoretical ACF seems reasonable for an EWMA type estimator of the variance.

In Fig. 9 we repeat the analysis for the DJIA in Section 2 but use the variance estimates for overlapping returns (5.2) instead. The construction of the plot is exactly as in Fig. 2. We see that the problem of spurious seasonality is no longer present and that the ten different variance series, shown in the upper graph of Fig. 9, do no longer show the slow change in their positions.

In contrast to Fig. 2, the pronounced sawtooth pattern in the series of daily variance estimates has vanished, as is evident from the lower graph in Fig. 9. Clearly, this has direct implications for the implied capital requirements of financial institutions. Considering again a long position in an equity instrument like the DJIA, risk measures like value-at-risk or expected shortfall, which are under certain assumptions proportional to the (conditional) volatility, will also no longer be prone to

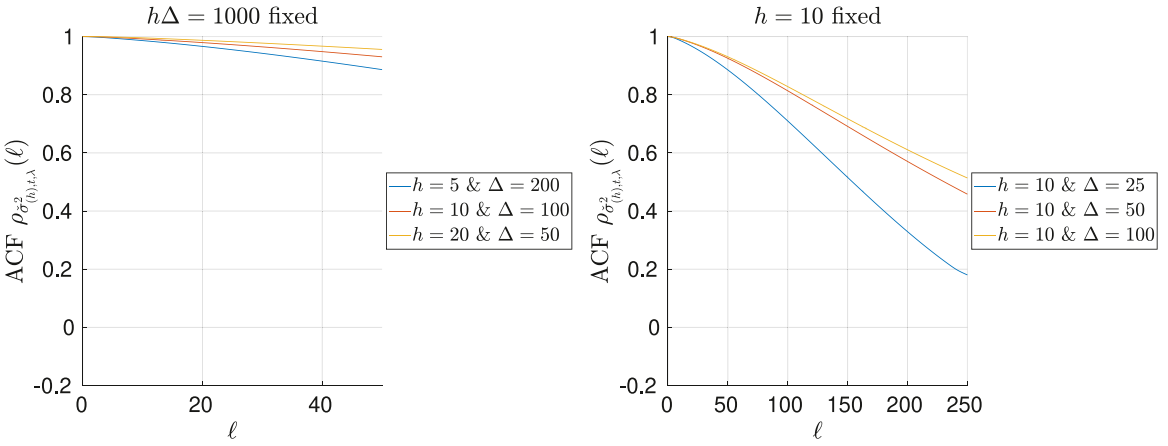

Fig. 8. The ACF of EWMA variances for overlapping returns (5.2), for daily returns from GARCH(1,1) process (4.7). For the left plot we use a fixed number of daily returns to derive the EWMA variances. The right plot depicts the ACF of EWMA variances based on bi-weekly ($h = 10$) returns and estimation windows $\Delta = 25, 50, 100$.

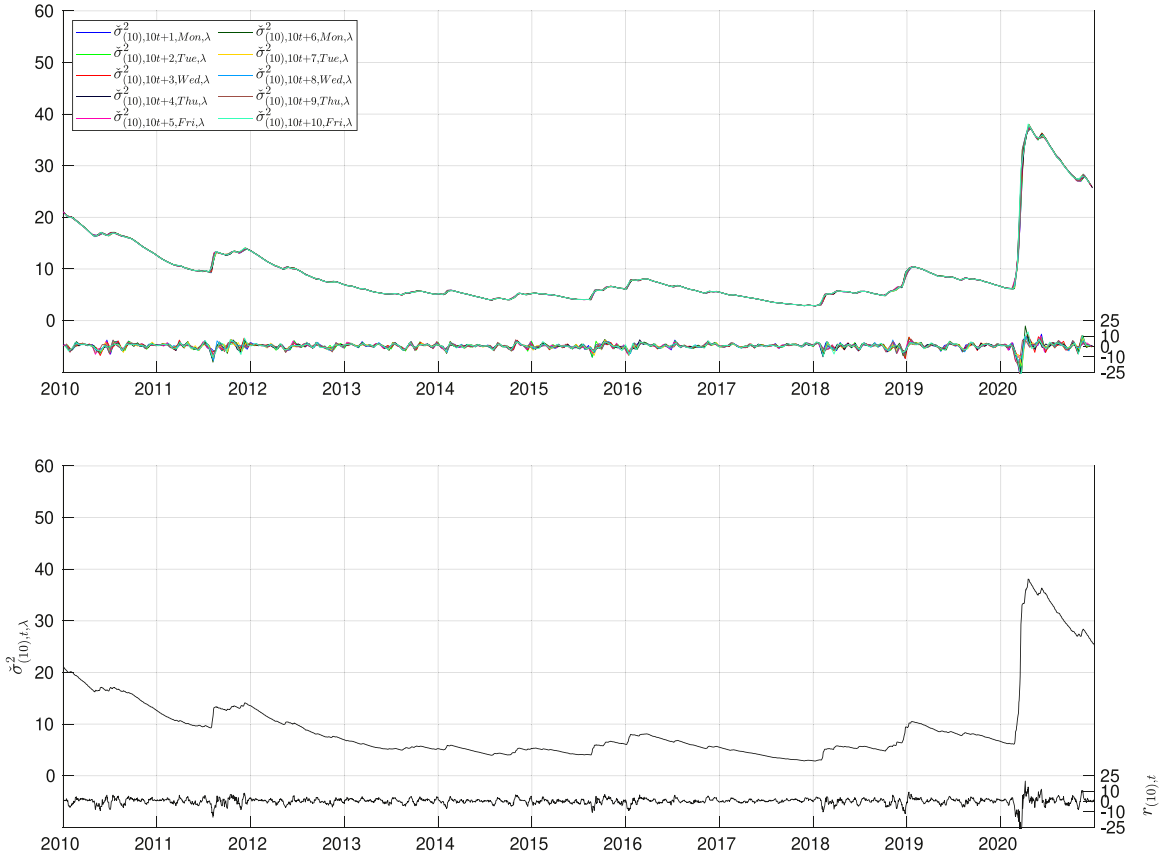

Fig. 9. Estimated EWMA variances for overlapping returns of the Dow Jones Industrial Average (DJIA) based on ten-day log-returns with a window length of 100 bi-weekly returns and an EWMA parameter of $\lambda = 0.96$. The first (last) estimates in both graphs are for 01-Jan-2010 (for 31-Dec-2020). The upper graph shows the ten series of bi-weekly variance estimates, each corresponding to a specific weekday and start date, and the lower graph the daily series of bi-weekly variance estimates. The corresponding ten-day log-returns are plotted at the bottom of both graphs with axis on the right.

exhibit spurious seasonality. This is a clear advantage of the variance estimator based on overlapping returns, as it largely alleviates or even avoids spurious behavior in risk-capital calculations. To fully assess the benefits in practice, empirical studies involving a realistic market portfolio would be in order. The consequences of spurious seasonality for backtesting procedures (cf. Christoffersen, 1998) to validate predictive risk models are also of interest for future research. Note however that, as pointed out by Kontaxis and Tsolas (2021), the autocorrelation structure of overlapping returns are a challenge for backtesting procedures. The procedures may need to be adapted in order to evaluate risk estimates with an assessment frequency that is more granular than the time horizon for risk assessment.

Another approach to avoid spurious seasonality is to simply take the average of the last h sample variances based on non-overlapping h-day returns. In the (ultra-)high-frequency context, this type of post-averaging of subsampling-based variance estimates has been proposed in Zhang et al. (2005) to overcome problems arising from microstructure noise. It is referred to as two-scales realized volatility and provides a consistent estimator of integrated volatility under the assumption of additive white noise. The two-scales variance estimator can also be written as a quadratic form and it can be interpreted as an estimator using overlapping return data. Graphical evidence (not shown here) indicates that also this estimator is not prone to spurious seasonality.

6. Concluding Remarks

We have investigated the phenomenon of spurious seasonality in sequentially estimated variances. It arises when the estimation frequency is higher than the sampling frequency of the (non-overlapping) return data used for estimation. The phenomenon, which, to our knowledge, has not yet been addressed in the literature, is attributable to an implicit overlap in the return data used for estimation. To provide a better understanding of this phenomenon, we have analyzed the properties of series of variance estimates in terms of their theoretical autocorrelation functions, considering a large class of DGPs and different variance estimators. We have shown ways to overcome the problem of spurious seasonality using overlapping return data. Our theoretical results are in line with the simulation-based results of Frankland et al. (2019), who, for risk assessment, favor overlapping data sampling combined with bias correction over non-overlapping data sampling.

In our analysis, we have focused exclusively on variance estimation. However, the phenomenon of spurious seasonality also translates directly to other risk measures, such as value-at-risk or expected shortfall, which are commonly used in order to determine the capital requirements of financial institutions. As a consequence, capital charges based on such risk estimates will be subject to spurious seasonality. Risk managers and regulators need to be aware of that phenomenon and, more importantly, understand it in order to establish sound risk management practices.

Our findings also provide an explanation for the variation in daily GARCH-parameter estimates derived from different non-overlapping monthly samples reported in Hedegaard and Hodrick (2016). Finally, although we have simplified our discussion by focusing on a daily data frequency, it should be understood that spurious seasonality also arises with other frequencies, such as in (ultra-)high-frequency realized-volatility analysis. Future research could address the phenomenon of spurious seasonality in multivariate settings, in the context of portfolio analysis and in the presence of time-varying GARCH structures.

Declaration of Competing Interest

The second author is co-founder and scientific advisor of Scalable Capital. Scalable Capital is a group of investment management and financial technology firms, which may or may not apply similar investment techniques or methods of analysis as described herein. The views expressed here are those of the authors and not necessarily those of Scalable Capital or its affiliates.

Acknowledgment

We thank the editor, the associate editor and two anonymous referees for their constructive comments and suggestions, which helped to greatly improve the manuscript. We are grateful for helpful comments from Michael Rockinger, Markus Glaser and participants of the 10th Annual Society for Financial Econometrics (SoFiE) Conference and the 8th CEQURA Conference on Advances in Financial and Insurance Risk Management.

Appendix A. Proofs of Results

A.1. Proof of Theorem 4.1

This follows directly from Lemma 6.2 in Magnus (1978).

A.2. Proof of Corollary 4.1

Let the daily returns, $(r_t)_t$, follow a Gaussian white noise process (Example 3.1) with $E[r_t] = 0$ and variances $\mathrm{Var}[r_t] = \sigma^2$. Then, $E[\boldsymbol{r}_{t,h\Delta+\ell}] = \mathbf{0}_{h\Delta+\ell}$ and $E[\boldsymbol{r}_{t,h\Delta+\ell}\boldsymbol{r}'_{t,h\Delta+\ell}] = \sigma^2\boldsymbol{I}_{h\Delta+\ell}$, so that, due to independence, the joint distribution of vec-

tor $\boldsymbol{r}_{t,h\Delta+\ell}$ is a multivariate normal distribution with zero mean vector and variance-covariance matrix $\sigma^2\boldsymbol{I}_{h\Delta+\ell}$. Using Theorem 4.1, it follows that

$$\operatorname{Cov}[\sigma^2_{(h),t},\sigma^2_{(h),t-\ell}] = 2\operatorname{tr}(\boldsymbol{KQK}'\sigma^2\boldsymbol{I}_{h\Delta+\ell}\boldsymbol{LQL}'\sigma^2 I_{h\Delta+\ell}) = 2\sigma^4\operatorname{tr}(\boldsymbol{KQK}'\boldsymbol{LQL}').$$

A.3. Proof of Theorem 4.2

For the covariance of the quadratic forms we get

$$\begin{aligned}
\operatorname{Cov}[\boldsymbol{X}'\boldsymbol{AX},\boldsymbol{X}'\boldsymbol{BX}] &= E[\boldsymbol{X}'\boldsymbol{AXX}'\boldsymbol{BX}] - E[\boldsymbol{X}'\boldsymbol{AX}]E[\boldsymbol{X}'\boldsymbol{BX}] \\
&= \sum_{i=1}^n\sum_{j=1}^n\sum_{k=1}^n\sum_{l=1}^n a_{ij}b_{kl}E[x_ix_jx_kx_l] - \operatorname{tr}(E[\boldsymbol{X}'\boldsymbol{AX}])\operatorname{tr}(E[\boldsymbol{X}'\boldsymbol{BX}]) \\
&= \sum_{i=1}^n\sum_{j=1}^n a_{ii}b_{jj}E[x_i^2x_j^2] + \sum_{i=1}^n\sum_{j=1,j\neq i}^n (a_{ij}b_{ij}+a_{ij}b_{ji})E[x_i^2x_j^2] - E[\operatorname{tr}(\boldsymbol{X}'\boldsymbol{AX})]E[\operatorname{tr}(\boldsymbol{X}'\boldsymbol{BX})] \\
&= \sum_{i=1}^n\sum_{j=1}^n (a_{ii}b_{jj}+\mathbb{1}_{\{i\neq j\}}2a_{ij}b_{ij})E[x_i^2x_j^2] - E[\operatorname{tr}(\boldsymbol{X}'\boldsymbol{AX})]E[\operatorname{tr}(\boldsymbol{X}'\boldsymbol{BX})] \\
&= E[\boldsymbol{X}^{2\odot\prime}\boldsymbol{CX}^{2\odot}] - E[\operatorname{tr}(\boldsymbol{AXX}')]E[\operatorname{tr}(\boldsymbol{BXX}')] \\
&= \operatorname{tr}(\boldsymbol{C}E[\boldsymbol{X}^{2\odot}\boldsymbol{X}^{2\odot\prime}]) - \operatorname{tr}(\boldsymbol{A}E[\boldsymbol{XX}'])\operatorname{tr}(\boldsymbol{B}E[\boldsymbol{XX}']) \\
&= \operatorname{tr}(\boldsymbol{C}(\boldsymbol{\Sigma}_{\boldsymbol{X}^{2\odot}} + \boldsymbol{\mu}_{\boldsymbol{X}^{2\odot}}\boldsymbol{\mu}'_{\boldsymbol{X}^{2\odot}})) - \operatorname{tr}(\boldsymbol{A\Sigma_X})\operatorname{tr}(\boldsymbol{B\Sigma_X}) \\
&= \operatorname{tr}(\boldsymbol{C\Sigma}_{\boldsymbol{X}^{2\odot}}) + \boldsymbol{\mu}'_{\boldsymbol{X}^{2\odot}}\boldsymbol{C\mu}_{\boldsymbol{X}^{2\odot}} - \operatorname{tr}(\boldsymbol{A\Sigma_X})\operatorname{tr}(\boldsymbol{B\Sigma_X}).
\end{aligned}$$

A.4. Proof of Corollary 4.2

From Theorem 4.2 we get

$$\gamma_{\sigma^2_{(h),t}}(\ell) = \operatorname{tr}(\boldsymbol{C}(\boldsymbol{\Sigma}_{\boldsymbol{r}^{2\odot}_{t,h\Delta+\ell}} + \boldsymbol{\mu}_{\boldsymbol{r}^{2\odot}_{t,h\Delta+\ell}}\boldsymbol{\mu}'_{\boldsymbol{r}^{2\odot}_{t,h\Delta+\ell}})) - \operatorname{tr}(\boldsymbol{KQK}'\boldsymbol{\Sigma}_{\boldsymbol{r}_{t,h\Delta+\ell}})\operatorname{tr}(\boldsymbol{LQL}'\boldsymbol{\Sigma}_{\boldsymbol{r}_{t,h\Delta+\ell}}),$$

with $\boldsymbol{C} = \boldsymbol{ab}' + 2(\boldsymbol{KQK}')\odot(\boldsymbol{LQL}')\odot(\boldsymbol{1}_{h\Delta+\ell}\boldsymbol{1}'_{h\Delta+\ell} - \boldsymbol{I}_{h\Delta+\ell})$, where $\boldsymbol{a} = \operatorname{diag}(\boldsymbol{KQK}')$ and $\boldsymbol{b} = \operatorname{diag}(\boldsymbol{LQL}')$. By assumption, $(r_t)_{t\in\mathbb{Z}}$ follows a weak white noise process (Definition 3.1) with zero mean, implying

$$\boldsymbol{\mu}_{\boldsymbol{r}^{2\odot}_{t,h\Delta+\ell}} = E[\boldsymbol{r}^{2\odot}_{t,h\Delta+\ell}] = \operatorname{Var}[r_t]\boldsymbol{1}_{h\Delta+\ell} = \sigma^2\boldsymbol{1}_{h\Delta+\ell}$$

and

$$\boldsymbol{\Sigma}_{\boldsymbol{r}_{t,h\Delta+\ell}} = E[\boldsymbol{r}_{t,h\Delta+\ell}\boldsymbol{r}'_{t,h\Delta+\ell}] = \operatorname{Var}[r_t]\boldsymbol{I}_{h\Delta+\ell} = \sigma^2\boldsymbol{I}_{h\Delta+\ell}.$$

Plugging in gives

$$\begin{aligned}
\gamma_{\sigma^2_{(h),t}}(\ell) &= \operatorname{tr}(\boldsymbol{C}(\boldsymbol{\Sigma}_{\boldsymbol{r}^{2\odot}_{t,h\Delta+\ell}} + \sigma^4\boldsymbol{1}_{h\Delta+\ell}\boldsymbol{1}'_{h\Delta+\ell})) - \sigma^4\operatorname{tr}(\boldsymbol{KQK}')\operatorname{tr}(\boldsymbol{LQL}') \\
&= \operatorname{tr}\big(\boldsymbol{C\Sigma}_{\boldsymbol{r}^{2\odot}_{t,h\Delta+\ell}}\big) + \sigma^4\big(\boldsymbol{1}'_{h\Delta+\ell}\boldsymbol{C1}_{h\Delta+\ell} - \operatorname{tr}(\boldsymbol{Q})^2\big).
\end{aligned}$$

Furthermore, with $\boldsymbol{A} := \boldsymbol{KQK}'$ and $\boldsymbol{B} := \boldsymbol{LQL}'$ we have

$$\begin{aligned}
\boldsymbol{1}'_{h\Delta+\ell}\boldsymbol{C1}_{h\Delta+\ell} &= \boldsymbol{1}'_{h\Delta+\ell}(\boldsymbol{ab}' + 2\boldsymbol{A}\odot\boldsymbol{B}\odot(\boldsymbol{1}_{h\Delta+\ell}\boldsymbol{1}'_{h\Delta+\ell} - \boldsymbol{I}_{h\Delta+\ell}))\boldsymbol{1}_{h\Delta+\ell} \\
&= \underbrace{\boldsymbol{1}'_{h\Delta+\ell}\boldsymbol{a}}_{=\operatorname{tr}(\boldsymbol{A})}\underbrace{\boldsymbol{b}'\boldsymbol{1}_{h\Delta+\ell}}_{=\operatorname{tr}(\boldsymbol{B})} + 2\boldsymbol{1}'_{h\Delta+\ell}(\boldsymbol{A}\odot\boldsymbol{B}\odot\boldsymbol{1}_{h\Delta+\ell}\boldsymbol{1}'_{h\Delta+\ell})\boldsymbol{1}_{h\Delta+\ell} - 2\boldsymbol{1}'_{h\Delta+\ell}(\boldsymbol{A}\odot\boldsymbol{B}\odot\boldsymbol{I}_{h\Delta+\ell})\boldsymbol{1}_{h\Delta+\ell} \\
&= \operatorname{tr}(\boldsymbol{Q})^2 + 2\boldsymbol{1}'_{h\Delta+\ell}(\boldsymbol{A}\odot\boldsymbol{B})\boldsymbol{1}_{h\Delta+\ell} - 2\boldsymbol{a}'\boldsymbol{b} \\
&= \operatorname{tr}(\boldsymbol{Q})^2 + 2\operatorname{tr}(\boldsymbol{AB}) - 2\boldsymbol{a}'\boldsymbol{b} \\
&= \operatorname{tr}(\boldsymbol{Q})^2 + 2\operatorname{tr}(\boldsymbol{KQK}'\boldsymbol{LQL}') - 2\boldsymbol{a}'\boldsymbol{b}.
\end{aligned}$$

This implies

$$\begin{aligned}
\gamma_{\sigma^2_{(h),t}}(\ell) &= \operatorname{tr}\big(\boldsymbol{C\Sigma}_{\boldsymbol{r}^{2\odot}_{t,h\Delta+\ell}}\big) + \sigma^4\big(\operatorname{tr}(\boldsymbol{Q})^2 + 2\operatorname{tr}(\boldsymbol{KQK}'\boldsymbol{LQL}') - 2\boldsymbol{a}'\boldsymbol{b} - \operatorname{tr}(\boldsymbol{Q})^2\big) \\
&= \operatorname{tr}\big(\boldsymbol{C\Sigma}_{\boldsymbol{r}^{2\odot}_{t,h\Delta+\ell}}\big) + 2\sigma^4\big(\operatorname{tr}(\boldsymbol{KQK}'\boldsymbol{LQL}') - \boldsymbol{a}'\boldsymbol{b}\big).
\end{aligned}$$

Appendix B. Additional Results and Figures

B.1. GARCH(p, q) Fulfills the Conditions of Corollary 4.2

Let $(r_t)_{t\in\mathbb{Z}}$, with $r_t = \sigma_t\varepsilon_t$, be a GARCH$(p,q)$ process as defined in Example 3.2. We further assume that the first four moments of r_t exist. Conditions for the existence of moments can be found in He and Teräsvirta (1999b) and Bollerslev (1986) for the GARCH(1,1) model and for the GARCH(p,q) model in Ling and McAleer (2002a). The functional form of the moments are given in He and Teräsvirta (1999a) and Karanasos (1999).

It is well known that GARCH processes are weak white noise processes (Definition 3.1), so it remains to show that the moment conditions (4.3)-(4.6) of Theorem 4.2 are satisfied. The first moment condition (4.3) is obviously fulfilled for the zero-mean process $(r_t)_{t\in\mathbb{Z}}$.

Let $\mathcal{I}_\tau := \{r_s : s \le \tau\}$. W.l.o.g. assume $t_1 < t_2 < t_3 < t_4$, then it holds

$$E[r_{t_1}r_{t_2}r_{t_3}r_{t_4}] = E[E[r_{t_1}r_{t_2}r_{t_3}r_{t_4}|\mathcal{I}_{t_4-1}]] = E[r_{t_1}r_{t_2}r_{t_3}\sigma_{t_4}E[\varepsilon_{t_4}|\mathcal{I}_{t_4-1}]] = 0,$$

which shows that moment condition (4.4) holds for GARCH(p,q) processes with symmetric innovation distributions and existing fourth moments. If $t_1 < t_2$, we obtain

$$E[r_{t_1}^3 r_{t_2}] = E[E[r_{t_1}^3 r_{t_2}|\mathcal{I}_{t_2-1}]] = E[r_{t_1}^3\sigma_{t_2}E[\varepsilon_{t_2}|\mathcal{I}_{t_2-1}]] = 0$$

and, if $t_1 > t_2$, it follows that

$$E[r_{t_1}^3 r_{t_2}] = E[E[r_{t_1}^3 r_{t_2}|\mathcal{I}_{t_1-1}]] = E[r_{t_2}\sigma_{t_1}^3E[\varepsilon_{t_1}^3|\mathcal{I}_{t_1-1}]] = 0,$$

showing that moment condition (4.5) holds for GARCH(p,q) processes with symmetric innovation distributions and existing fourth moments. Let $t_1 < \max\{t_2,t_3\}$ and w.l.o.g. $t_3 > t_2$, then

$$E[r_{t_1}^2 r_{t_2}r_{t_3}] = E[E[r_{t_1}^2 r_{t_2}r_{t_3}|\mathcal{I}_{t_3-1}]] = E[r_{t_1}^2 r_{t_2}\sigma_{t_3}E[\varepsilon_{t_3}|\mathcal{I}_{t_3-1}]] = 0.$$

W.l.o.g. assume $q \ge 3$, otherwise set $\alpha_r = 0$ for $r > q$ in the following derivation. If $t_1 > \max\{t_2,t_3\}$, $E[\varepsilon_t^2] = \sigma^2$ and w.l.o.g. $t_1 = t$, $t_2 = t-1$ and $t_3 = t-2$, we have

$$\begin{aligned}
E[r_{t_1}^2 r_{t_2}r_{t_3}] &= E[r_t^2 r_{t-1}r_{t-2}] = E[E[r_t^2 r_{t-1}r_{t-2}|\mathcal{I}_{t-1}]] = E[r_{t-1}r_{t-2}E[\sigma_t^2\varepsilon_t^2|\mathcal{I}_{t-1}]] \\
&= E[r_{t-1}r_{t-2}\sigma_t^2E[\varepsilon_t^2]] = \sigma^2E[r_{t-1}r_{t-2}(\alpha_0 + \sum_{i=1}^{q}\alpha_i r_{t-i}^2 + \sum_{j=1}^{p}\beta_j\sigma_{t-j}^2)] \\
&= \sigma^2\alpha_0E[r_{t-1}r_{t-2}] + \sigma^2\sum_{j=1}^{p}\beta_jE[r_{t-1}r_{t-2}\sigma_{t-j}^2] + \sigma^2\alpha_1E[r_{t-1}^3r_{t-2}] + \sigma^2\alpha_2E[r_{t-1}r_{t-2}^3] \\
&\quad + \sigma^2\sum_{i=3}^{q}\alpha_iE[r_{t-1}r_{t-2}r_{t-i}^2] \\
&= \sigma^2\sum_{j=1}^{p}\beta_jE[r_{t-2}\sigma_{t-j}^2\sigma_{t-1}E[\varepsilon_{t-1}|\mathcal{I}_{t-1}]] \\
&= 0,
\end{aligned}$$

which shows that moment condition (4.6) holds for GARCH(p,q) processes with symmetric innovation distributions and existing fourth moments.

B.2. Gaussian White Noise Process with the Sample Variance

Figs. 10 and 11 in this section of the appendix are analogous to Figs. 4 and 5 but with GARCH(1,1) (4.7) being replaced by Gaussian white noise as DGP and the EWMA variance (3.4) being substituted by the sample variance (3.3).

B.3. Functional Form and Amplitude of the Periodic Spurious Seasonality in the Theoretical ACF

The theoretical autocovariance function of the quadratic-form variance estimator, when the daily log-return process, $(r_t)_{t\in\mathbb{Z}}$, is a weak white noise process satisfying the moment conditions (4.3)-(4.6), is given in Corollary 4.2 for $\ell \ge 0$ by

$$\gamma_{\sigma^2_{(h),t}}(\ell) = \operatorname{tr}\big(\boldsymbol{C}\boldsymbol{\Sigma}_{\boldsymbol{r}^{2\odot}_{t,h\Delta+\ell}}\big) + 2\sigma^4\big(\operatorname{tr}(\boldsymbol{K}\boldsymbol{Q}\boldsymbol{K}'\boldsymbol{L}\boldsymbol{Q}\boldsymbol{L}') - \boldsymbol{a}'\boldsymbol{b}\big),$$

with $\boldsymbol{C} = \boldsymbol{a}\boldsymbol{b}' + 2(\boldsymbol{K}\boldsymbol{Q}\boldsymbol{K}')\odot(\boldsymbol{L}\boldsymbol{Q}\boldsymbol{L}')\odot(\mathbf{1}_{h\Delta+\ell}\mathbf{1}_{h\Delta+\ell}' - \boldsymbol{I}_{h\Delta+\ell})$, where $\boldsymbol{a} = \operatorname{diag}(\boldsymbol{K}\boldsymbol{Q}\boldsymbol{K}')$ and $\boldsymbol{b} = \operatorname{diag}(\boldsymbol{L}\boldsymbol{Q}\boldsymbol{L}')$. The expression is rather compact, but lacks intuition. It is not obvious where exactly the spurious seasonality is coming from and how the

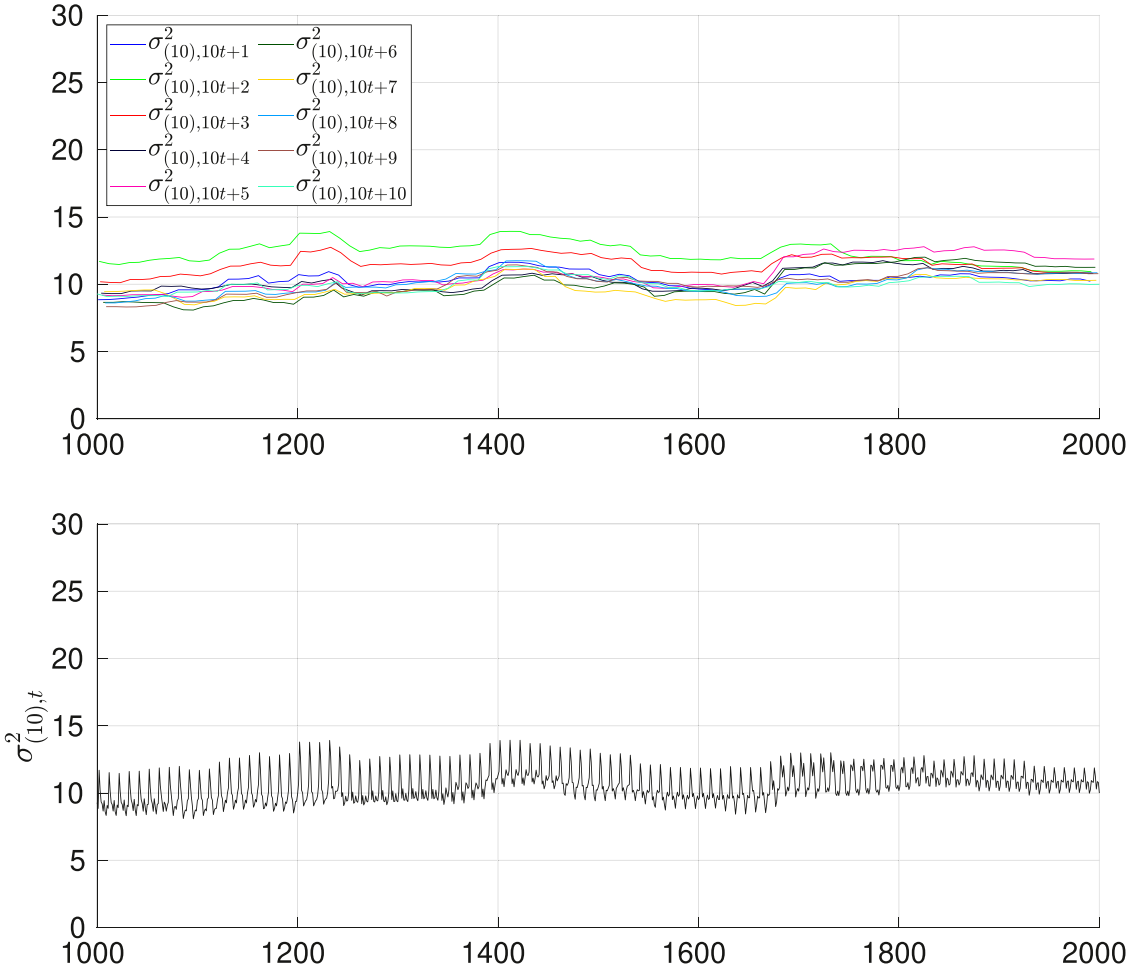

Fig. 10. Time series of sample variance estimates (3.3), $\sigma^2_{(h),t}$, for simulated daily return series from the Gaussian white noise process with variance $\sigma^2 = 1$. The upper plot shows the estimates $(\sigma^2_{(10),10t+\tau})_{t\in\mathbb{Z}}$, for $1 \le \tau \le 10$. The lower plot shows the series $(\sigma^2_{(10),t})_{t\in\mathbb{Z}}$. Both plots are based on bi-weekly ($h = 10$) returns and estimation window $\Delta = 100$.

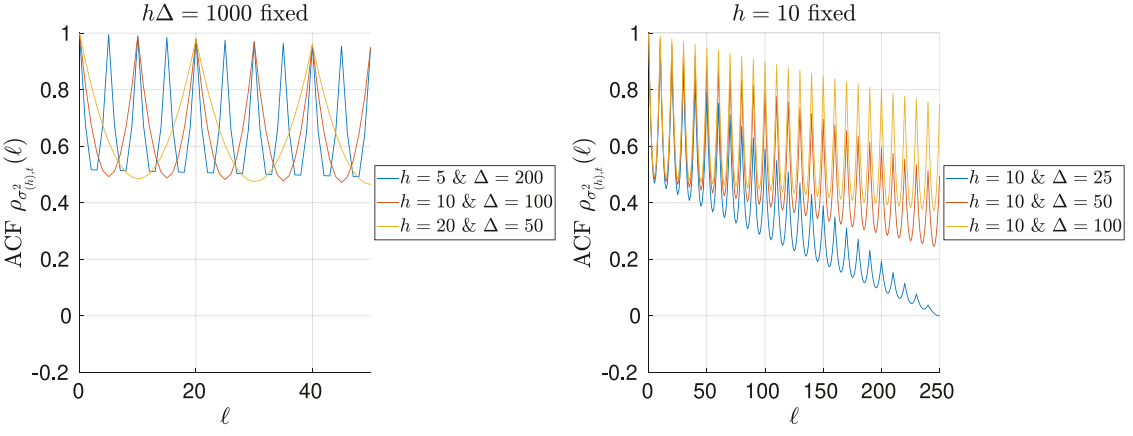

Fig. 11. The ACF of sample variances (3.3), $\sigma^2_{(h),t}$, for daily returns from the Gaussian white noise process with $\sigma^2 = 1$. For the left plot we use a fixed number of daily returns to derive the sample variances. The right plot depicts the ACF of sample variances based on bi-weekly ($h = 10$) returns and estimation windows $\Delta = 25, 50, 100$.

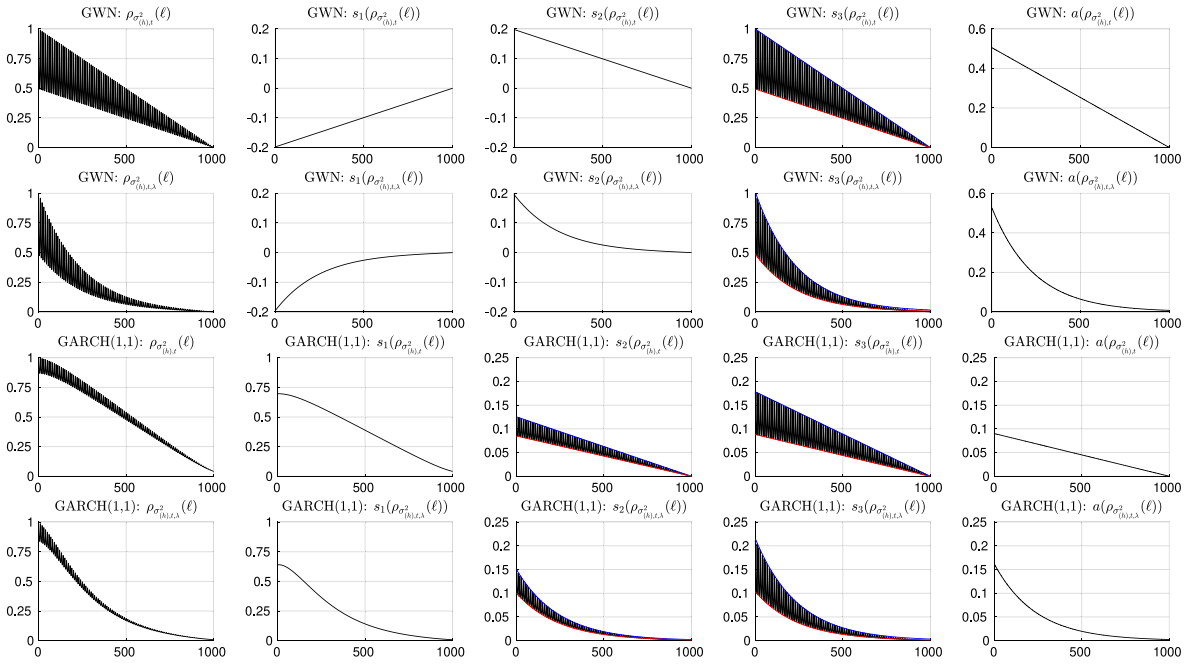

Fig. 12. The ACF, its components $s_1(\cdot)$, $s_2(\cdot)$, $s_3(\cdot)$, and peak-to-peak amplitudes, $a(\cdot)$, of sample variances (first and third row), $\sigma^2_{(h),t}$, and EWMA variances (second and fourth row), $\sigma^2_{(h),t,\lambda}$, for different lags ℓ. The time-scale on the horizontal axis represents lags of ℓ days. In the first two rows, for the daily returns a Gaussian white noise process with $\sigma^2 = 1$ is assumed and in the third and fourth row the GARCH(1,1) process (4.7). All plots are based on bi-weekly ($h = 10$) returns and estimation window $\Delta = 100$.

amplitude of the periodic spurious seasonality in the theoretical ACF depends on the variance estimator and the DGP. To provide more insight, we re-write the theoretical autocovariance as a sum of three components

$$\gamma_{\sigma^2_{(h),t}}(\ell) = s_1(\mathbf{Q}) + s_2(\mathbf{Q}) + s_3(\mathbf{Q}),$$

with

$$\begin{aligned}
s_1(\mathbf{Q}) &:= \boldsymbol{b}'\boldsymbol{\Sigma}_{\mathbf{r}^{2\odot}_{t,h\Delta+\ell}}\boldsymbol{a} - 2(\sigma^4 + \gamma_{r_t^2}(0))\boldsymbol{a}'\boldsymbol{b},\\
s_2(\mathbf{Q}) &:= 2\mathrm{tr}\Big(((\boldsymbol{K}\boldsymbol{Q}\boldsymbol{K}') \odot (\boldsymbol{L}\boldsymbol{Q}\boldsymbol{L}'))\boldsymbol{\Sigma}_{\mathbf{r}^{2\odot}_{t,h\Delta+\ell}}\Big),\\
s_3(\mathbf{Q}) &:= 2\sigma^4\mathbf{1}'_{h\Delta+\ell}((\boldsymbol{K}\boldsymbol{Q}\boldsymbol{K}') \odot (\boldsymbol{L}\boldsymbol{Q}\boldsymbol{L}'))\mathbf{1}_{h\Delta+\ell}.
\end{aligned}$$

The three terms depend on the variance estimator defining $\mathbf{Q}$ and the DGP, which impacts σ^4, $\gamma_{r_t^2}(0)$ and $\boldsymbol{\Sigma}_{\mathbf{r}^{2\odot}_{t,h\Delta+\ell}}$. In the following we consider again the Gaussian white noise process with $\sigma^2 = 1$ and GARCH(1,1) process (4.7). As variance estimators, we study the sample variance and the EWMA variance based on non-overlapping h-day returns with $h = 10$. The window length is set to $\Delta = 100$.

Fig. 12 shows the theoretical ACF of the estimated variances, $\rho_{\sigma^2_{(h),t}}(\ell)$ and the three components $s_i(\rho_{\sigma^2_{(h),t}}(\ell)) = s_i(\mathbf{Q}_{(h),\Delta})/\gamma_{\sigma^2_{(h),t}}(0)$. Note that the components add up to the theoretical ACF, i.e., $\rho_{\sigma^2_{(h),t}}(\ell) = \sum_{i=1}^3 s_i(\rho_{\sigma^2_{(h),t}}(\ell))$. The two top rows correspond to the Gaussian white noise process with the sample variance in the first row and the EWMA variance in the second row. Accordingly, the third and fourth row show the results for the GARCH(1,1) process and the respective variance estimators. We see that the first component $s_1(\rho_{\sigma^2_{(h),t}}(\ell))$ is not contributing to the periodic spurious seasonality effect and the functional form depends on the variance estimator and the DGP. The second component, $s_2(\rho_{\sigma^2_{(h),t}}(\ell))$, is not periodic for the Gaussian white noise process but periodic for the GARCH(1,1) process. This is due to the fact that $\boldsymbol{\Sigma}_{\mathbf{r}^{2\odot}_{t,h\Delta+\ell}}$ is diagonal for Gaussian white noise but not for GARCH(1,1) processes, since squared observations are autocorrelated. In case of the sample variance, the peak-to-peak amplitude in $s_2(\rho_{\sigma^2_{(h),t}}(\ell))$ is decreasing more slowly than for the EWMA variance estimator. The third term, $s_3(\rho_{\sigma^2_{(h),t}}(\ell))$, is periodic in all four cases and the functional form of the amplitude is comparable to those of the second component. The fifth column shows the contribution of the second and third component to the peak-to-peak amplitudes, denoted by $a(\rho_{\sigma^2_{(h),t}}(\ell))$. The peak-to-peak amplitudes have been approximated by fitting linear

functions (for the sample variance) and exponential functions (for the EWMA variance) through the peaks and taking the pointwise differences between the fitted functions. The fitted curves are shown in blue and red in the plots of $s_2(\cdot)$ and $s_3(\cdot)$. We see that the peak-to-peak amplitude of the sample variance is decreasing in ℓ, and it is larger for the Gaussian white noise process than for the GARCH(1,1) process. The peak-to-peak amplitudes for the EWMA variances are comparable to those of the sample variance for small values of ℓ, but the amplitudes are decreasing much faster in ℓ.

The crucial term in both periodic components, $s_2(\boldsymbol{Q})$ and $s_3(\boldsymbol{Q})$, is $(\boldsymbol{KQK}') \odot (\boldsymbol{LQL}')$. The block-structure of $\boldsymbol{Q}_{(h),\Delta,\lambda}$ and $\boldsymbol{Q}_{(h),\Delta}$ and the fact that $\boldsymbol{KQK}' = \text{blkDiag}(\boldsymbol{0}_{\ell\times\ell}, \boldsymbol{Q})$ and $\boldsymbol{LQL}' = \text{blkDiag}(\boldsymbol{Q}, \boldsymbol{0}_{\ell\times\ell})$ have a block-diagonal structure reveal how the periodicity of length h is generated, when different lags, ℓ, are considered and the Hadamard product of the matrices $\boldsymbol{KQK}'$ and $\boldsymbol{LQL}'$ is formed.

References

Andersen, T.G., Bollerslev, T., 1998. Answering the skeptics: Yes, standard volatility models do provide accurate forecasts. International Economic Review 39 (4), 885–905.
Andersen, T.G., Bollerslev, T., Lange, S., 1999. Forecasting financial market volatility: Sample frequency vis-à-vis forecast horizon. Journal of Empirical Finance 6 (5), 457–477.
BCBS, 2016. Minimum capital requirements for market risk. http://www.bis.org/bcbs/publ/d352.htm.
BCBS, 2019. Minimum capital requirements for market risk. https://www.bis.org/bcbs/publ/d457.htm.
Bod, P., Blitz, D., Franses, P.H., Kluitman, R., 2002. An unbiased variance estimator for overlapping returns. Applied Financial Economics 12 (3), 155–158.
Bollerslev, T., 1986. Generalized autoregressive conditional heteroskedasticity. Journal of Econometrics 31 (3), 307–327.
Britten-Jones, M., Neuberger, A., Nolte, I., 2011. Improved inference in regression with overlapping observations. Journal of Business Finance & Accounting 38 (56), 657–683.
Chan, W.-S., 2022. On temporal aggregation of some nonlinear time-series models. Econometrics and Statistics 21, 38–49.
Christoffersen, P.F., 1998. Evaluating interval forecasts. International Economic Review 39 (4), 841–862.
Christoffersen, P.F., Diebold, F.X., Schuermann, T., 1998. Horizon problems and extreme events in financial risk management. Economic Policy Review 4 (3), 109–118.
Daníelsson, J., James, K.R., Valenzuela, M., Zer, I., 2016. Model risk of risk models. Journal of Financial Stability 23, 79–91.
Daníelsson, J., Zigrand, J.-P., 2006. On time-scaling of risk and the square-root-of-time rule. Journal of Banking & Finance 30 (10), 2701–2713.
Diebold, F.X., Hickman, A., Inoue, A., Schuermann, T., 1997. Converting 1-day volatility to h-day volatility: Scaling by h is worse than you think. Wharton Financial Institutions Center, Working Paper 97-34.
Drost, F.C., Nijman, T.E., 1993. Temporal aggregation of GARCH processes. Econometrica 61 (4), 909–927.
Embrechts, P., Kaufmann, R., Patie, P., 2005. Strategic long-term financial risks: Single risk factors. Computational Optimization and Applications 32 (1), 61–90.
Engle, R.F., 1982. Autoregressive conditional heteroscedasticity with estimates of the variance of united kingdom inflation. Econometrica 50 (4), 987–1007.
Frankland, R., Smith, A.D., Sharpe, J., Bhatia, R., Jarvis, S., Jakhria, P., Mehta, G., 2019. Calibration of VaR models with overlapping data. British Actuarial Journal 24, 1–30.
Hansen, L.P., Hodrick, R.J., 1980. Forward exchange rates as optimal predictors of future spot rates: An econometric analysis. Journal of Political Economy 88 (5), 829–853.
He, C., Silvennoinen, A., Teräsvirta, T., 2008. Parameterizing unconditional skewness in models for financial time series. Journal of Financial Econometrics 6 (2), 208–230.
He, C., Teräsvirta, T., 1999a. Fourth moment structure of the GARCH(p,q) process. Econometric Theory 15, 824–846.
He, C., Teräsvirta, T., 1999b. Properties of moments of a family of GARCH processes. Journal of Econometrics 92 (1), 173–192.
Hedegaard, E., Hodrick, R.J., 2016. Estimating the risk-return trade-off with overlapping data inference. Journal of Banking & Finance 67, 135–145.
Horváth, L., Kokoszka, P., Zitikis, R., 2006. Sample and implied volatility in GARCH models. Journal of Financial Econometrics 4 (4), 617–635.
Karanasos, M., 1999. The second moment and the autocovariance function of the squared errors of the GARCH model. Journal of Econometrics 90 (1), 63–76.
Kluitman, R., Franses, P.H., 2002. Estimating volatility on overlapping returns when returns are autocorrelated. Applied Mathematical Finance 9 (3), 179–188.
Kole, E., Markwat, T., Opschoor, A., van Dijk, D., 2017. Forecasting value-at-risk under temporal and portfolio aggregation. Journal of Financial Econometrics 15 (4), 649–677.
Kontaxis, G., Tsolas, I.E., 2021. Evaluation of backtesting techniques on risk models with different horizons. Journal of Risk Model Validation 15, 29–50.
Kontaxis, G., Tsolas, I.E., 2022. Evaluation of backtesting on risk models based on data envelopment analysis. Journal of Operational Risk 17, 51–79.
Kuester, K., Mittnik, S., Paolella, M.S., 2006. Value-at-Risk Prediction: A Comparison of Alternative Strategies. Journal of Financial Econometrics 4 (1), 53–89.
Ling, S., McAleer, M., 2002a. Necessary and sufficient moment conditions for the GARCH(r,s) and asymmetric power GARCH(r,s) models. Econometric Theory 18, 722–729.
Ling, S., McAleer, M., 2002b. Stationarity and the existence of moments of a family of GARCH processes. Journal of Econometrics 106 (1), 109–117.
Longerstaey, J., & Spencer, M., 1996. RiskMetrics™—Technical Document. J.P.Morgan/Reuters, New York.
Magnus, J.R., 1978. The moments of products of quadratic forms in normal variables. Statistica Neerlandica 32 (4), 201–210.
McNeil, A.J., Frey, R., 2000. Estimation of tail-related risk measures for heteroscedastic financial time series: an extreme value approach. Journal of Empirical Finance 7 (3–4), 271–300.
Mittnik, S., 1988. Derivation of the theoretical autocovariance and autocorrelation function of autoregessive moving average processes. Communications in Statistics - Theory and Methods 17 (11), 3825–3831.
Mittnik, S., 2011. Solvency II calibrations: Where curiosity meets spuriosity. Center for Quantitative Risk Analysis (CEQURA), Working Paper Number 04.
Nelson, D.B., Cao, C.Q., 1992. Inequality constraints in the univariate GARCH model. Journal of Business & Economic Statistics 10 (2), 229–235.
Silvestrini, A., Veredas, D., 2008. Temporal aggregation of univariate and multivariate time series models: A survey. Journal of Economic Surveys 22 (3), 458–497.
Sun, H., Nelken, I., Han, G., Guo, J., 2009. Error of VAR by overlapping intervals. Asia Risk April 2009, 50–55. https://www.risk.net/risk-management/1509219/error-var-overlapping-intervals
Taylor, S., Fang, M., 2018. Unbiased weighted variance and skewness estimators for overlapping returns. Swiss Journal of Economics and Statistics 154 (21), 1–8.
Tsai, H., Chan, K.-S., 2008. A note on inequality constraints in the GARCH model. Econometric Theory 24 (3), 823–828.
Williamson, S. H., 2021. Daily closing values of the DJA in the United States, 1885 to present. MeasuringWorth, URL: https://www.measuringworth.com/datasets/DJA/, accessed 15-Jan-2021.
Zhang, L., Mykland, P.A., Aït-Sahalia, Y., 2005. A tale of two time scales. Journal of the American Statistical Association 100 (472), 1394–1411.
Zinde-Walsh, V., 1988. Some exact formulae for autoregressive moving average processes. Econometric Theory 4 (3), 384–402.